Review

Comparative study of photocatalytic activity of metals- and non-metals doped ZnO and TiO2 nanocatalysts for advanced photocatalysis

Hamad AlMohamadi , Sameer A. Awad , Ashwani Kumar Sharma * , Normurot Fayzullaev , Arístides Távara-Aponte , Lincoln Chiguala-Contreras , Abdelfattah Amari , Carlos Rodriguez-Benites , Mohamed A. Tahoon , Hossein Esmaeili *

Posted Date: 11 June 2024

doi: 10.20944/preprints202406.0592.v1

Keywords: Zinc oxide; Titanium dioxide; Photocatalysis; Dopants; Organic contaminants; Wastewater

Review

Comparative Study of Photocatalytic Activity of Metals- and Non-Metals Doped ZnO and TiO_2 Nanocatalysts for Advanced Photocatalysis

Hamad AlMohamadi [1,2], Sameer A. Awad [3], Ashwani Kumar Sharma [4,*], Normurot Fayzullaev [5], Arístides Távara-Aponte [6], Lincoln Chiguala-Contreras [7], Abdelfattah Amari [8], Carlos Rodriguez-Benites [9], Mohamed A. Tahoon [10,11] and Hossein Esmaeili [12,*]

1 Department of Chemical Engineering, Faculty of Engineering, Islamic University of Madinah, Madinah, Saudi Arabia,
2 Sustainability Research Center, Islamic University of Madinah, Madinah, Saudi Arabia; hha@iu.edu.sa
3 Department of Medical Laboratories Techniques, Al-Maarif University College, Ramadi, Iraq; sameer.msc1981@gmail.com
4 Department of Applied Sciences, Chandigarh Engineering College, Chandigarh Group of Colleges, Jhanjeri, Mohali 140307, Punjab, India; Ashwani2.research@cgcjhanjeri.in
5 Department of Polymer Chemistry and Chemical Technology, University Samarkand State University, Samarkand, 140101, Uzbekistan; nfayzullaev1972@gmail.com
6 Departamento Académico de Física, Universidad Nacional de Trujillo, Trujillo, Perú; stavara@unitru.edu.pe
7 Universidad Nacional Agraria de la Selva, Tingo Maria, Perú; lincoln.chiguala@unas.edu.pe
8 Department of Chemical Engineering, College of Engineering, King Khalid University, Abha 61411, Kingdom of Saudi Arabia; abdelfattah.amari@enig.rnu.tn
9 Universidad de Ciencias y Artes de América Latina, Av. La Molina 3755, Lima, 15026, Perú; carlosrbfisica@gmail.com
10 1 Department of Chemistry, College of Science, King Khalid University, P.O. Box 9004, Abha 61413, Saudi Arabia; tahooon_87@yahoo.com
11 Chemistry Department, Faculty of Science, Mansoura University, Mansoura 35516, Egypt
12 Department of Chemical Engineering, Bushehr, Branch, Islamic Azad University, Bushehr, Iran
* Correspondence: esmaeili.hossein@gmail.com; Tel.: +989179885692

Abstract: This review article provides useful information on TiO_2 and ZnO photocatalysts and their derivatives in removing organic contaminants such as different types of dyes, hydrocarbons, pesticides, etc. Also, the reaction mechanism of TiO_2 and ZnO photocatalysts and their derivatives was investigated. In addition, the impact of adding metallic (e.g., Ag, Co, Pt, Pd, Cu, Au, Ni) and non-metallic (e.g., C, N, O, S) dopants to their structure on the photodegradation efficiency of organic compounds was thoroughly studied. Moreover, advantages and disadvantages of various synthesis procedures of ZnO and TiO_2 nanocatalysts were discussed and compared. Furthermore, the impact of photocatalyst dosage, photocatalyst structure, contaminant concentration, pH, light intensity and wavelength, temperature and reaction time on the photodegradation efficiency was studied. According to previous studies, adding metallic and non-metallic dopants to the TiO_2 and ZnO structure led to a remarkable enhance in their stability and reusability. Besides, doped TiO_2 and ZnO demonstrated remarkable photocatalytic efficiencies in eliminating various types of organic contaminants.

Keywords: zinc oxide; titanium dioxide; photocatalysis; dopants; organic contaminants; wastewater

1. Introduction

Water scarcity has recently become a major problem owing to global warming, rapid industrial growth, depletion of water resources, environmental pollution, and uncontrolled development of groundwater [1,2]. The rapid industrial growth after the Industrial Revolution has remarkably increased living standard, but threatens human health [3]. Because of the development and growth

 doi:10.20944/preprints202406.0592.v1

of industries, industrial effluents are becoming more polluted and difficult to treat. The release of organic compounds and chemical fertilizers from various industries has polluted river water and has become increasingly a global pollution [4]. Moreover, complete removal of non-biodegradable organic contaminants is tough using biological treatment technologies [5]. Biological processes are safe, economical, and reliable, but the removal percentage of suspended solids is low, so they need better operation management [6]. The coagulation and precipitation techniques can suspend solid particles with formation of flocs after adding polymeric coagulant and/or inorganic coagulant (such as Al, Fe, etc.). Coagulants bind solids together to form larger particles (flocs), then the flocs settle and separate from the effluent. This method has a high purification performance, but utilizing chemicals and generating biological sludge cause blockage of pipes and water deterioration, thus limit the use of this process [7,8]. In the Fenton oxidation process, organic compounds are broken down using a strong oxidizer reagent. OH radicals can be produced by oxidizer reagents through a reaction between H_2O_2 and iron salts. This process is easy to apply and additional equipment is not utilized excessively in comparison to other oxidation processes or photo-oxidation process. However, this process has some drawbacks such as sludge production and high operating costs for secondary process [9,10].

An advanced water treatment process can purify water at a high rate and effectively eliminate pollutants [11]. Advanced Oxidation Technology utilizes various techniques for enhancement of oxidation power. For efficient water refinement, various contaminants must be removed economically [12]. Generally, various active species can play a key role in the photocatalytic reaction, including superoxide radicals ($O_2^{\bullet -}$), holes (h^+), and hydroxyl radicals ($^\bullet OH$) [13]. Advanced technology using TiO_2 and ZnO photocatalysts has attracted the most attention for producing $OH^\bullet$ using optical energy without additional chemicals. Also, the operating cost of this technique may be significantly decreased by solar energy. The low photocatalytic performance of ZnO and TiO_2 may limit the practical application of advanced technology to treat wastewater [14]. Numerous studies have been done on modifying their surface by metal and non-metal dopants for their possible practical utilization [15].

Various analyzes characterize the structure of ZnO and TiO_2 nanocatalysts, including XRD for determining crystal phases and crystal size, AFM for determining refractive index profiles, FTIR for specifying the functional groups, and EDX for determining the constituents. All these features are critical in the photocatalytic reaction. Also, SEM and TEM analyses are used to characterize the morphology and appearance structure of a catalyst [16,17]. Figure 1 demonstrates SEM and TEM photos of ZnO and TiO_2 nanocatalysts. As shown, ZnO and TiO_2 have various morphologies, shapes and sizes.

 doi:10.20944/preprints202406.0592.v1

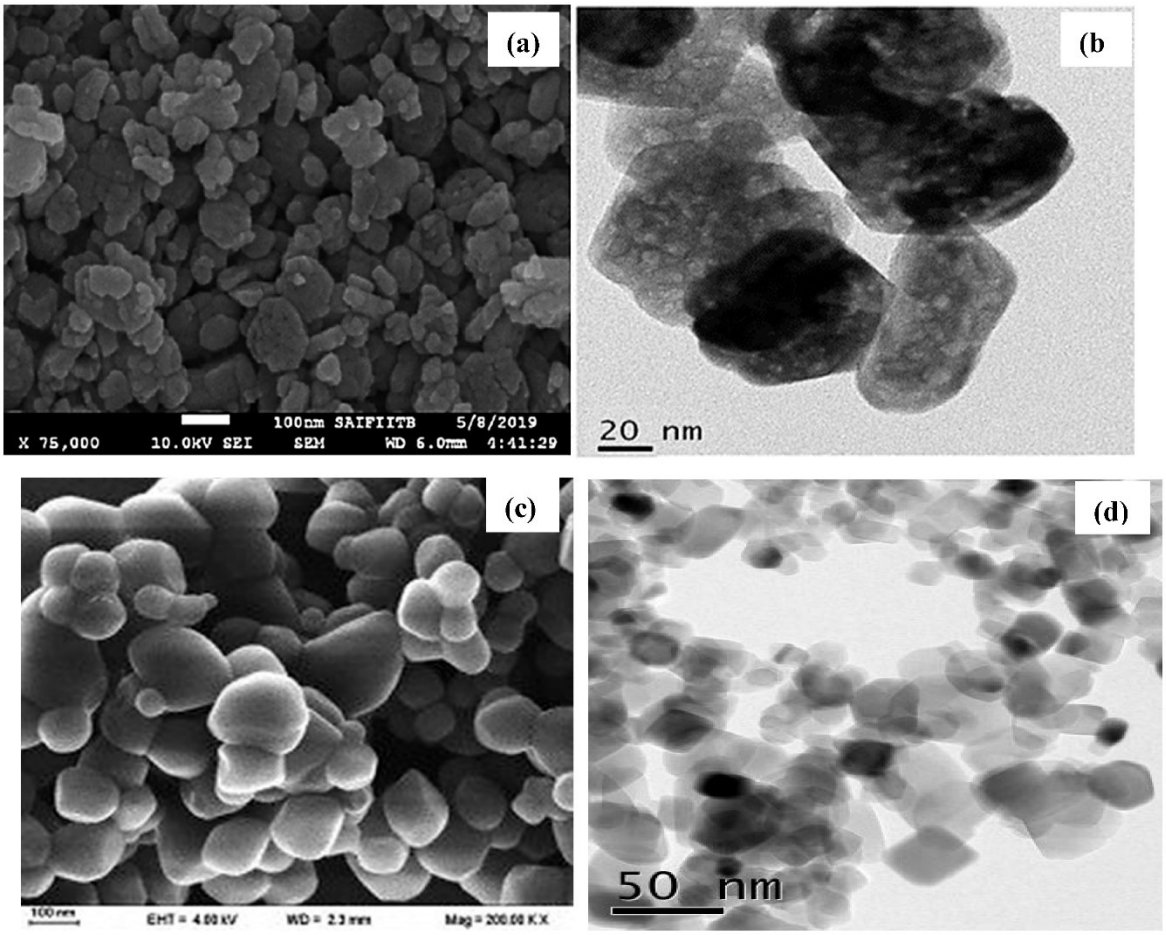

Figure 1. SEM and TEM images of ZnO (a-b) [18] and TiO_2 (c-d) [19].

TiO_2 and ZnO photocatalysts are extensively utilized for photodegradation of contaminants under UV light or sunlight. However, owing to their band gap range, they have limitations for the photodegradation of pollutants. For doing so, TiO_2 and ZnO photocatalysts can be combined with other compounds to synthesize an efficient photocatalyst, some of which include La/TiO_2 [20], CuO/WO_3/TiO_2 [21], Fe_3O_4/TiO_2 [22], carbon-doped TiO_2 [23], N,P-codoped carbon quantum dots/TiO_2 [24], Fe_3O_4/CuO/ZnO/graphene [25], rGO/Fe_3O_4/ZnO [26], tungsten/silver/ZnO [27], Pb/ZnO, Cd/ZnO, Ag/ZnO [28], and Bi(12)ZnO(20) [29].

The paper focuses on comparing the photocatalytic capability of TiO_2 and ZnO and their composites in the degradation of organic compounds in wastewater. Also, the advantages, disadvantages, and structural features of these photocatalysts were thoroughly investigated. Moreover, the photodegradation mechanism of contaminants using TiO_2 and ZnO as well as metals-doped and non-metals doped TiO_2 and ZnO were completely discussed. Furthermore, the photodegradation efficiency of different contaminants using these photocatalysts and their derivatives (metallic- and non-metallic- dopants in their structure) were compared. One of the main features of catalysts is their stability in the photocatalytic reaction, so the recyclability of TiO_2 and ZnO and their composites was fully studied.

2. Organic Pollutants

Municipal sewage pollutants are mainly organic matter and a variety of pathogenic microorganisms and so on with complex structures such as drugs, antioxidants, polycyclic aromatic hydrocarbons, pharmaceutical intermediates, food additives, PPCPs, steroids, and phenolic compounds [30]. Also, pollutants in industrial wastewaters include gas condensates [5], petroleum products, non-chlorinated compounds, petroleum hydrocarbons, trinitrotoluene, and polycyclic

 doi:10.20944/preprints202406.0592.v1

aromatic hydrocarbon [31]. The presence of hydrocarbon compounds in wastewater causes many problems for human health. Discharge of these wastewaters to sea must be performed under certain conditions. The highest permissible concentration of hydrocarbon compounds for discharge into the sea should be 40 ppm, and TDS less than 32000 ppm [32].

Another kind of contaminants in wastewater is volatile organic compounds (VOCs), which have destructive effects on human health. Volatile organic contaminants are categorized into 3 groups, including semi volatile organic compounds (SVOCs), volatile organic compounds (VOCs), and very volatile organic compounds (VVOCs). Propane and butane are some VVOCs, which are poisonous compounds in very low concentrations. VOCs are also toxic compounds found in household products and environment, including isopropyl alcohol, acetone, formaldehyde, toluene, vinyl chloride, and hexanal. Molecular weight and boiling point of SVOCs are higher than VOCs and can evaporate at room temperature. Pesticides such as chlordane and plasticizers such as phthalates are some of the SVOCs [33]. The utmost allowable limit of organic compounds for drainage into the river for utilization in agricultural irrigation should be less than 200 ppm [34].

The main source of VOCs includes incomplete burning of fossil fuels, solvents used in inks and paints (e.g., acetone, ethyl acetate, and glycol ether), utilizing biofuels (e.g., cooking oil and bioethanol), biomass combustion, especially from agricultural residuals, and VOCs released from metal working fluids [33]. The presence of these contaminants in sewages results in various problems for the environment.

Also, tetracycline, sulfamethoxazole, cefixime, amoxicillin, gentamicin, erythromycin, and ciprofloxacin are kinds of antibiotics that are present in hospital effluents. The presence of antibiotics in effluents in low and high concentrations is dangerous and causes serious damage to human health. According to reports, the concentration of antibiotics in surface and groundwater reaches 100 micrograms per liter. Also, the concentration of amoxicillin in raw effluent and urban wastewater treatment is 171 mg/L and 13 ng/L, respectively [35]. The acceptable standard of WHO for antibiotics in wastewater is 1 mg/L [36]. Therefore, their concentrations in wastewater should be attenuated.

Dyes are another kind of organic compounds, which are utilized in many industries like food, plastics, paper, cosmetics and textile. Among these, the most abundant dyes are related to the textile industry, which these dyes can enter the wastewater [37]. More than 7×10^5 tons of dyes are produced annually, 10–15% of which enters the sewage during the dyeing process. Water pollution by dyes results in many environmental problems. The highest allowable limit of dyes in industrial discharge is in the range 0.01 to 0.05 mg/L. Different groups of dyes are considered carcinogens or mutants. Dyes can prevent sunlight from entering the water, and disrupting biological process in the water. Most dyes are poisonous to organisms and have adverse impacts on their aquatic life, and entire ecosystem. The presence of dye in water causes reproductive dysfunction, kidney damage, carcinogenesis and mutagenicity. Basic dyes are cationic dyes and most of them are crystalline compounds, which can be derived from positively charged sulfur or nitrogen atoms. Under visible and UV light irradiation, dyes have high stability and insensitivity, and do not degrade without photocatalyst [38-40]. Cationic, anionic and non-ionic are 3 important categories of dyes, among which, the toxicity of cationic dyes is more than the other two. There are various types of dyes in sewage including crystal violet, Congo Red (CR), methyl orange (MO), reactive orange, reactive black, reactive red, methylene blue (MB), methyl violet, brilliant cresyl blue and Safranin-T that may be generated by plastic, leather, food dye, printing, paper, and textile industries [41,42]. Figure 2 illustrates different categories of organic compounds with some examples.

 doi:10.20944/preprints202406.0592.v1

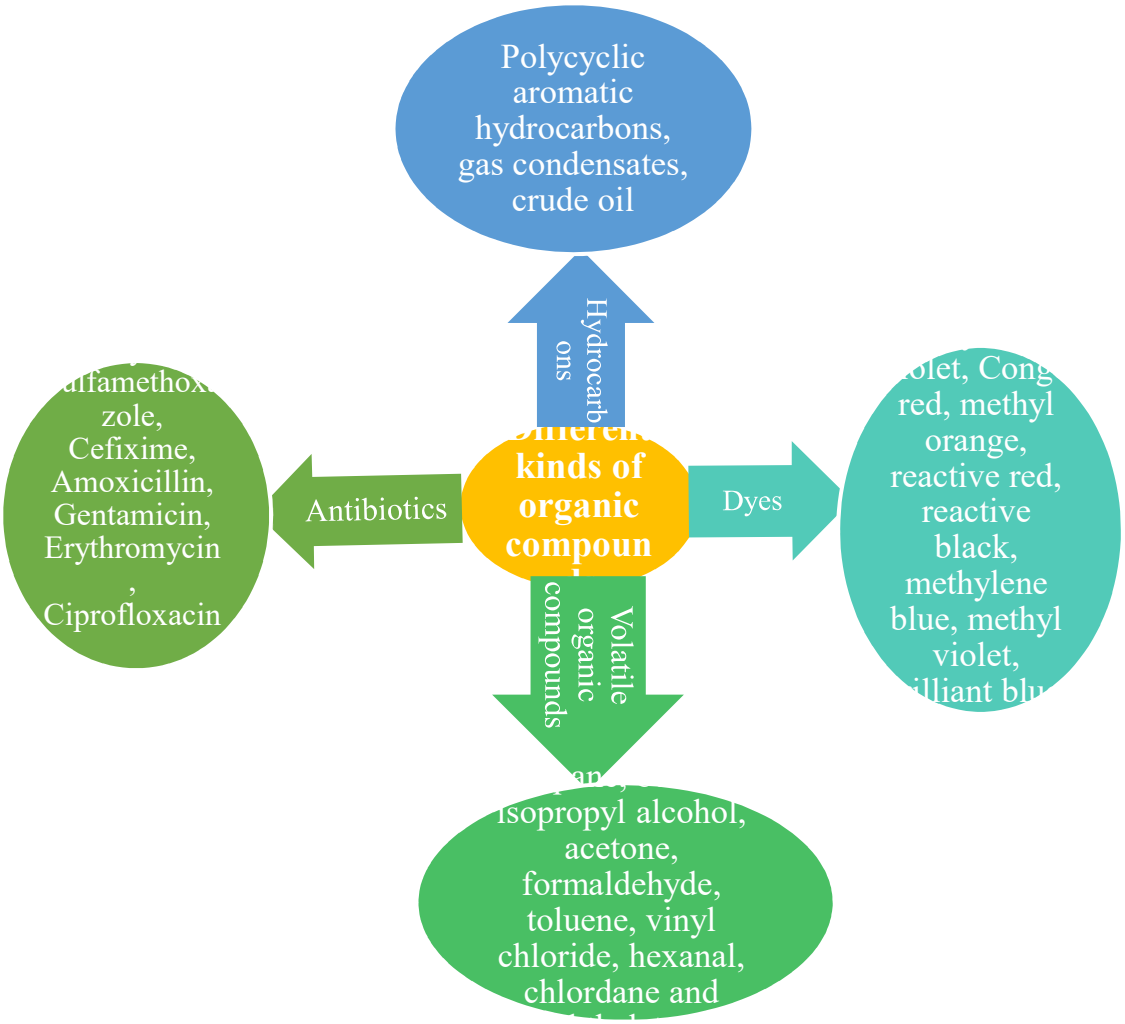

Figure 2. Different categories of organic compounds.

3. TiO_2 Photocatalyst

TiO_2 is a non-toxic and insoluble substance in water. TiO_2 has high stability with a high catalytic performance. Another name of TiO_2 is Titania, which can be available in 3 forms such as anatase, brookite, and rutile [43,44]. The rutile (tetragonal) crystalline structure of TiO_2 is quite stable in particles greater than 35 nm [45]. TiO_2 in anatase and rutile structures have oxidation strengths of 3-3.2 eV, respectively, which are very strong oxidation strengths [14]. One of the most important applications of TiO_2 is its utilization in the photocatalytic process. To this end, UV light, halogen lamp or solar irradiation can help accelerate the photocatalytic reaction in the presence of TiO_2 nanocatalyst [46]. The photocatalyst has two important properties. For instance, the photocatalyst should not be consumed or participate directly in the reaction. Also, the photocatalyst provides other mechanism pathways. Photocatalytic reaction is based on the absorption of solar energy in the semiconductor gap. Few semiconductors can be utilized as the catalyst in the photocatalysis process, of which, TiO_2 is the most extensively utilized [44]. The various morphologies of TiO_2 consist of zero, one, two and three-dimensional structures. By optimization of the shape and size, the photocatalytic activity of TiO_2 particles in the wastewater treatment process can be maximized [47].

TiO_2 can be synthesized easily by various physical, chemical, and thermal procedures such as chemical or physical vapor deposition, sol-gel, inverse micelle, solvothermal, hydrothermal, sonochemical, microwave, and electrodeposition process [48]. Synthesizing metal-doped semiconductor oxides by conventional physical mixing or chemical deposition usually obtains

 doi:10.20944/preprints202406.0592.v1

insoluble materials that are inherently difficult to control the morphology, size, and dispersing metal components. These methods need long time and multi-stage processes. Sonochemistry procedure is an efficient process for preparing mesoporous materials. Ultrasound is very useful to synthesize an extensive range of nanostructured materials, which include high-specific surface area oxides, alloys, carbides, and transition metals [15]. Neppolian et al. synthesized TiO_2 nanophotocatalysts by a combination of ultrasonic and sol–gel processes. They investigated the impact of various factors on the synthesis method, including magnetic stirring, ultrasonic sources (e.g., bath and horn), ultrasonic time, power density, temperature, and reactor size [49]. Table 1 indicates the advantages and disadvantages of various processes for TiO_2 synthesis. As shown, the production of high-quality crystals as well as easy control of crystals in TiO_2 can be achieved by hydrothermal process. Also, the fabrication of TiO_2 with sol-gel process has several benefits such as high purity products, good size distribution, remarkable specific surface area, economical, uniform size of particles, fine particle size, and simple synthesis. Between these processes, utilizing the microwave method has significant benefits such as short reaction time, high reaction rate and high efficiency.

Table 1. Advantages and disadvantages of various techniques for TiO_2 fabrication.

Process	Advantages and disadvantages	Ref.
Hydrothermal	Advantages: Good size distribution, crystal shape control, low defects, synthesizing large crystals with high quality, fine particle size Disadvantages: high equipment cost, high temperature and pressure needed, long synthesis time	[50]
Sol-gel	Advantages: High purity products, good size distribution, remarkable specific surface area, economical, uniform size of particles, fine particle size, ease of synthesis Disadvantages: agglomeration of particles, long processing time, using organic solvents which may be toxic	[50]
Flame pyrolysis	Advantages: Rapid and mass production Disadvantages: Requires high energy, ease of rutile formation	[48]
Solvothermal	Advantages: High crystallinity, suitability for materials, low defects, better control of the features of TiO_2 compared to hydrothermal process Disadvantages: requires organic solvents, unstable at high temperature	[48,51]
Inverse micelle	Advantages: Fine particle sizes, high crystallinity, low defects Disadvantages: High cost, high crystallization temperature	[48]
Sonochemical	Advantages: High-specific surface area, simple control of particles and morphology, efficient for mesoporous materials, improve reaction rate, short time, no additive Disadvantages: Low yield, inefficient energy	[15,50]
Microwave heating	Advantages: Fast heating, short reaction time, high reaction rate and efficiency	[51]

3.1. Features and Reaction Mechanism of TiO_2 Photocatalyst

Utilization of TiO_2 as a photocatalyst for elimination of contaminants from wastewater has several benefits, which include: 1) the process is done at room temperature and 1 atm, 2) complete decontamination without secondary contamination, 3) producing high surface area and high catalytic activity, and 4) using the photocatalyst in multiple cycles and decreasing the costs [52]. The decomposition process of contaminants is mainly an oxidative reaction, which depends on the features of the photocatalyst. TiO_2 is also low-cost, suitable band gap energy, long-term stability against light, and safe. Generally, the band distance and wavelength of TiO_2 are between 3-3.2 eV, and 400 nm, respectively, indicating that UV light at a wavelengths less than 400 nm leads to an inverse reaction. Also, UV irradiation at a wavelength less than 400 nm initiates a photoreaction. Unfavorable recombination of holes (h^+) and electrons (e^-), and low yield in the visible region under irradiation are 2 important disadvantages of TiO_2 [15]. The catalytic activity of TiO_2 photocatalyst can be enhanced under UV irradiation, because TiO_2 uses only 5% of the solar energy [53].

 doi:10.20944/preprints202406.0592.v1

At UV light<400 nm, the surface of TiO_2 may reach temperatures above 30000°C, which this temperature can oxidize all substances. Hence, all organic compounds are completely decomposed into CO_2 and water. Figure 3(a) illustrate a schematic of degradation of contaminants by forming photo-induced charge carriers electron/hole (e^-/h^+) on the TiO_2 surface. Also, Figure 3(b) shows that the catalyst surface is surrounded by the contaminant molecules. On the TiO_2 surface, oxygen molecules react with electrons to produce oxygen radicals. Also, water molecules react with h^+ for generating hydroxide radicals and H^+ ions. The final products will be CO_2 and H_2O [14]. In other words, electrons introduced into the conduction band from valence band can be easily transferred to the catalyst surface and are trapped by doping with noble metals, intermediate metals, and rare earth elements. Metal-doped cations increase the ability of radicals produced in the photocatalysis reaction and then decrease the recombination life of e^-/h^+ [54].

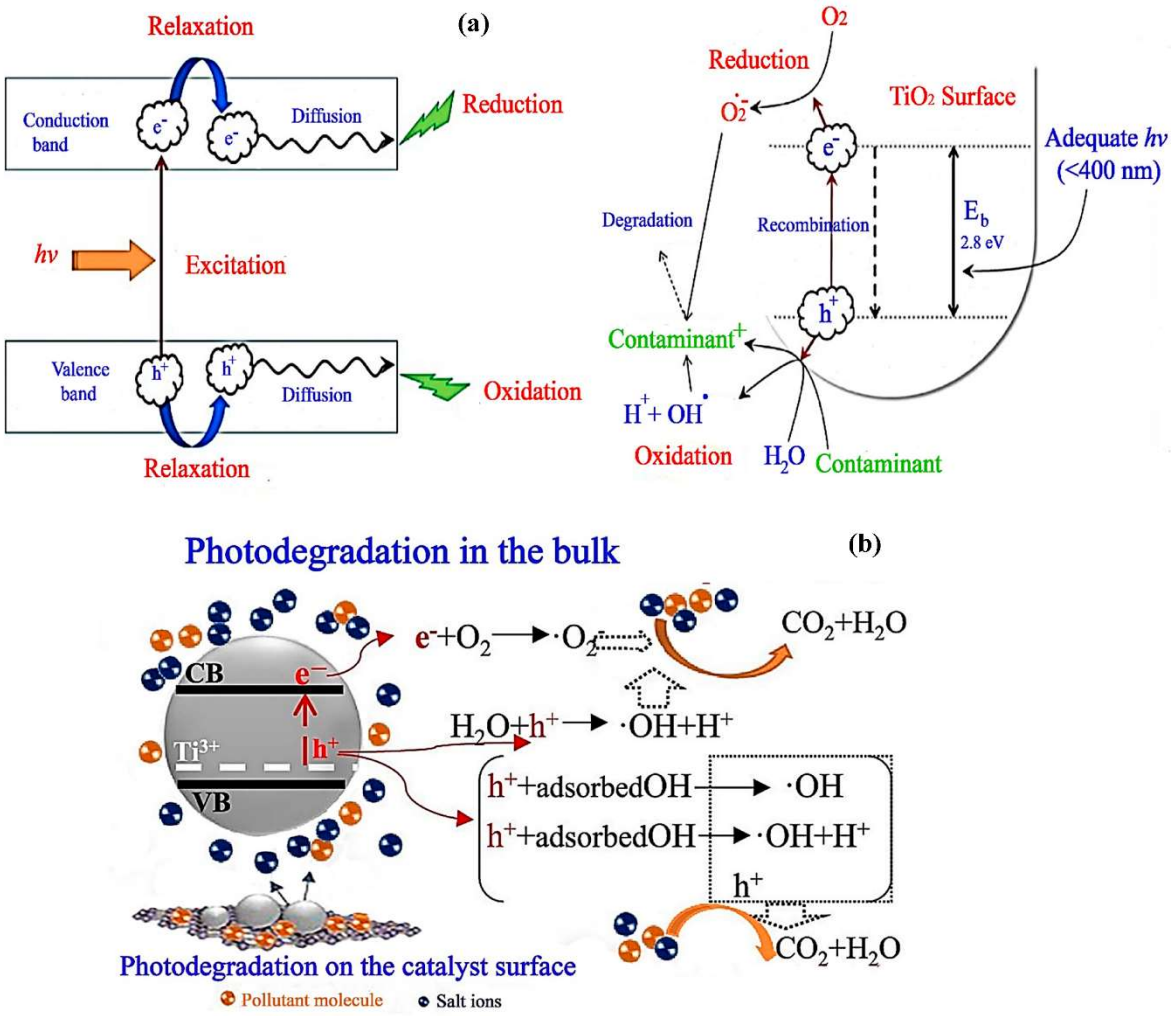

Figure 3. Photoinduced charge carriers (e^-/h^+) generation on the TiO_2 surface for eliminating contaminants (a) and photodegradation of contaminants on the TiO_2 surface (b).

By irradiating UV light to the TiO_2 surface, the photo-induced electrons react with dissolved oxygen for producing $O_2^{\bullet}$. The photoinduced h^+ in the valence band penetrate to the surface of the TiO_2 photocatalyst and react with the absorbed water molecules to form $OH^{\bullet}$. $OH\bullet$ is a highly active species in the photocatalytic process. The reaction mechanism of TiO_2 and the electron–hole pair is defined as follows. As shown, TiO_2 reacts with $h\upsilon$ to produce e^- and h^+. Next, e^- and h^+ can produce two important radicals such as $OH^{\bullet}$ and $O_2^{\bullet}$, which have important role in the photocatalytic reaction [14,54].

$$TiO_2 + h\upsilon \rightarrow TiO_2(\ e^-_{CB} + h^+_{VB})$$

 doi:10.20944/preprints202406.0592.v1

Oxidation: $e_{CB}^{-}+H_2O \rightarrow OH^{\bullet}+H^{+}$

Reduction: $O_2 + e_{CB}^{-} \rightarrow O_2^{\bullet}$

$$e_{CB}^{-}+ HO_2^{\bullet} \rightarrow HO_2^{-}$$

$$h_{VB}^{+} + HO_2^{-} \rightarrow H_2O_2$$

$$TiO_2(h^+) + H_2O_{ads} \rightarrow TiO_2 + HO_{ads}^{\cdot} + H^+$$

$$TiO_2(h^+) + HO^- \rightarrow TiO_2 + HO_{ads}^{\cdot}$$

$$TiO_2(e^-) + O_2 \rightarrow TiO_2 + O_2^{\cdot}$$

$$O_2^{\cdot -} + H_2O \rightarrow HO_2^{\cdot} + HO^-$$

$$O_2^{\bullet} + H^+ \rightarrow HO_2^{\bullet}$$

$$2HO_2^{\cdot} \rightarrow H_2O_2 + O_2$$

$$TiO_2(e^-) + H_2O_2 \rightarrow TiO_2 + HO^- + HO^{\cdot}$$

$$TiO_2(h^+) + R_{ads} \rightarrow TiO_2 + R_{ads}^{+}$$

where, R is the adsorbed pollutant [55].

Also, TiO_2 is photochemically stable and non-toxic. Under irradiation, the charge-pair on TiO_2 reacts directly with solid lattice ions. Also, TiO_2 is resistant to various acidic and alkaline pHs. TiO_2 can be utilized in the photocatalytic treatment of the environment. Hence, TiO_2 can be used as a promising photocatalyst to degrade organic contaminants. Nevertheless, TiO_2 particles are inactive in visible light. To solve this problem, numerous studies have been performed on the synthesis of various composites of TiO_2 with metals and non-metals (e.g., ceramics, zeolites, carbon materials, fibers and glasses) as a support in order to have photocatalytic activity in a wide range of visible light [14].

The recombination behavior of e^-/h^+ decrease with decreasing the size of TiO_2 NPs, which can be because of the increase in interfacial charge transfer at TiO_2 surfaces. Also, the photocatalytic activity of TiO_2 of less than a few nanometers decreases because of the predominant recombination of electron/hole at the TiO_2 surface. According to the reports, TiO_2 nanotubes are more effective in degrading contaminants than TiO_2 particles, indicating the rapid mass transfer of contaminants on the surface of nanotubes [45].

3.2. Improved Photocatalytic Activity of TiO_2 Using Metallic and Non-Metallic Dopants

As mentioned earlier, TiO_2 photocatalyst can decompose organic contaminants under UV irradiation. Researchers have tried to improve the optical sorption range of TiO_2 catalysts from ultraviolet irradiation to visible light to boost its photocatalytic activity. Therefore, for improving the photocatalytic activity of TiO_2 in visible lights, its surface should be modified [56]. The catalytic activity of TiO_2 can be improved by placing suitable materials on the surface of TiO_2 for its application under visible irradiation [53,57,58]. Metallic particles such as Pd, Pt, Fe, Ru, Au, and Ag can be utilized on the TiO_2 surface to improve the photocatalytic activity by suppressing recombination behaviors of e^-/h^+. The induced electrons migrate to the surface of metal particles, stabilizing the photo-induced h^+ on TiO_2 as the life time of the charge carrier increases. To this end, more superoxide ($O_2^{\bullet}$) and $OH^{\bullet}$ radicals can be produced. As the crystallographic aspects of TiO_2 increase, the photocatalytic activity of TiO_2 also produces more OH•, which can contribute to the photodegradation of organic pollutants. Also, the element O in the lattice of TiO_2 may be replaced by

 doi:10.20944/preprints202406.0592.v1

various heteroatoms such as B, S, F, N, P, and common doping B-C and N-S to perform a photocatalytic reaction in the presence of visible light. Besides, metals and non-metals introduced to the TiO_2 structure can improve its catalytic activity for the decomposition of organic pollutants [14,59]. Also, modifying the surface of TiO_2 improves the uptake capacity of contaminants, which can be useful in advanced oxidation technology. The modified TiO_2 with nanotubes, foams, and mesoporous phases has shown better photocatalytic behavior compared to unmodified TiO_2 [60].

TiO_2 photocatalyst on a nanoscale has a great surface area/volume proportion, leading to increased charge separation and ions trapping at the TiO_2 surface. TiO_2 nanoparticles show enhanced oxidative power compared to TiO_2 microparticles. However, TiO_2 nanocatalyst can not be employed directly to wastewater treatment owing to the aggregation of particles during the degradation process as well as their physical and chemical features. To this end, the catalytic activity of TiO_2 NPs can be improved by incorporating TiO_2 onto carbon materials for composite synthesis such as graphene, carbon nanotubes, and activated carbon nanofiber. Carbon materials can be excellent supports for TiO_2 NPs owing to their unique features like excellent mechanical, thermal, chemical, electrical, and optical properties, which lead to rapid charge transfer on the surface of TiO_2/carbon nanocomposites [61]. TiO_2/carbon nanocomposites are suitable catalysts for the elimination of organic contaminants from effluents. Graphene NPs act as a bridge for excellent electron transfer and electron sinks. TiO_2/graphene nanocomposites have an extensive range of band gap (2.66–3.18 eV), suggesting that long-wavelength lights in the visible region can be absorbed by the TiO_2/carbon nanocomposite. One of the most benefits of carbon nanomaterials is their high specific surface area, in which TiO_2 NPs may be distributed in their structure, leading to improved selectivity of organic contaminants. TiO_2/carbon nanocomposite has a good impact on self-purification in comparison to UV irradiation and ozonation when used for wastewater treatment. These nanocomposites can be effective industrially for wastewater purification because carbon NPs are employed as a support to stabilize the composite structure [62].

The photocatalytic activity of TiO_2 can be enhanced by enhancing the interfacial charge-transfer and reducing the recombination of e^-/h^+. To this end, various metals can be used to improve the photocatalytic activity of TiO_2, including Ag, boron (B), Si, Ni, and so on under UV light or sun light irradiation. Generally, there are several ways for improving the photocatalytic activity of TiO_2, including enhancing the ratio of surface/volume, integrating TiO_2 with other semiconductors, optimizing its particle size, and doping metals or non-metals. The presence of metal dopants in the TiO_2 structure remarkably affects the photo-reactivity because by shifting the catalyst band gap to the visible region, it changes the interfacial electron transfer rate and the charge-carrying recombination rate [63]. A dopant ion can trap e^- or h^+, leading to longer lifespan of the produced charge carriers and increased photocatalytic activity. Figure 4 indicates various dopants used in the TiO_2 structure. As shown, transition metals, anionic compounds, metal oxides and transition metal ceramics are the main dopants for improving the TiO_2 surface. Fe, Al, Zr, Co, Cu, and Ni are several types of transition metals. Also, Fe_2O_3, Cr_2O_3, and SiO_2 are the most important metal oxides. Moreover, WO_3, SnO_2, and MoO_3 are the most important transition metal ceramics. Eventually, C, N, F, O, and S are non-metallic dopants. The addition of transition metals to the TiO_2 surface can enhance its catalytic activity and decline the recombination of photogenerated e^- and h^+ [15]. The photodegradation mechanism of contaminants using metals- and non-metals- doped TiO_2 is also illustrated in Figure 5 [64,65]. As shown, the presence of metals and non-metals on the TiO_2 surface can help improve its photocatalytic activity by producing more oxygen radicals. These oxygen radicals play a key role in photodegradation of organic contaminants.

 doi:10.20944/preprints202406.0592.v1

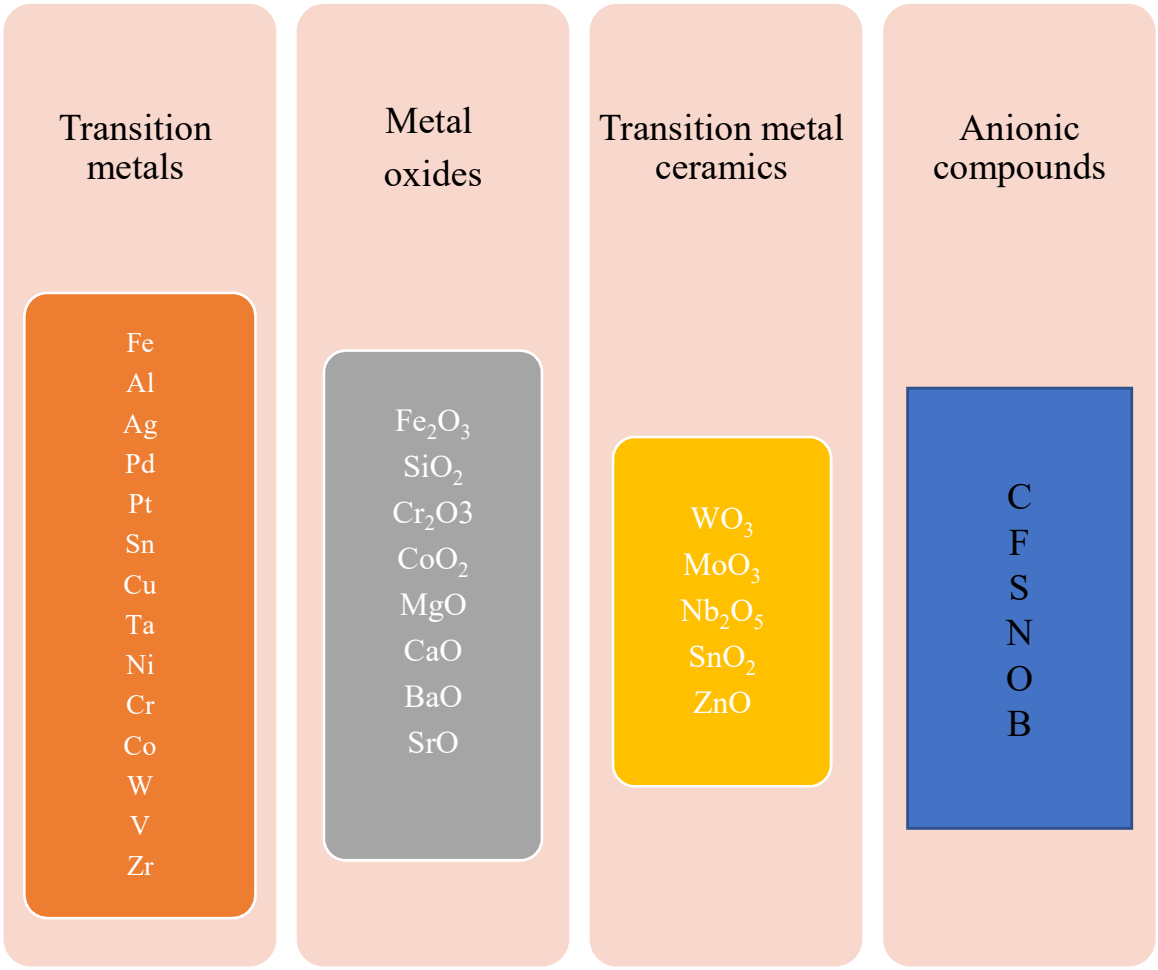

Figure 4. Types of dopants used in the TiO_2 structure

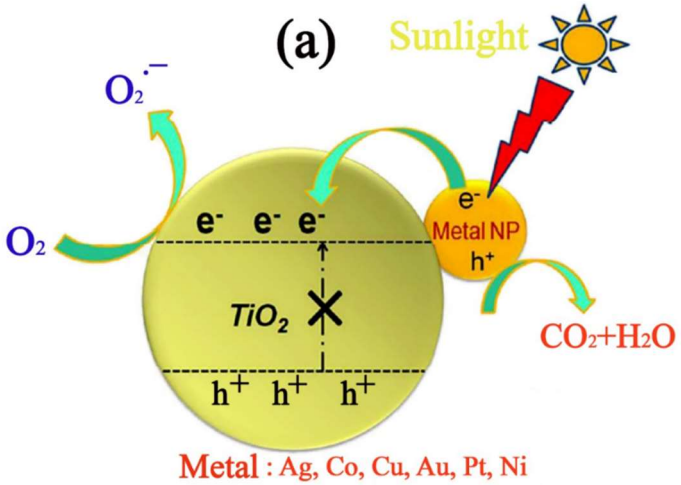

 doi:10.20944/preprints202406.0592.v1

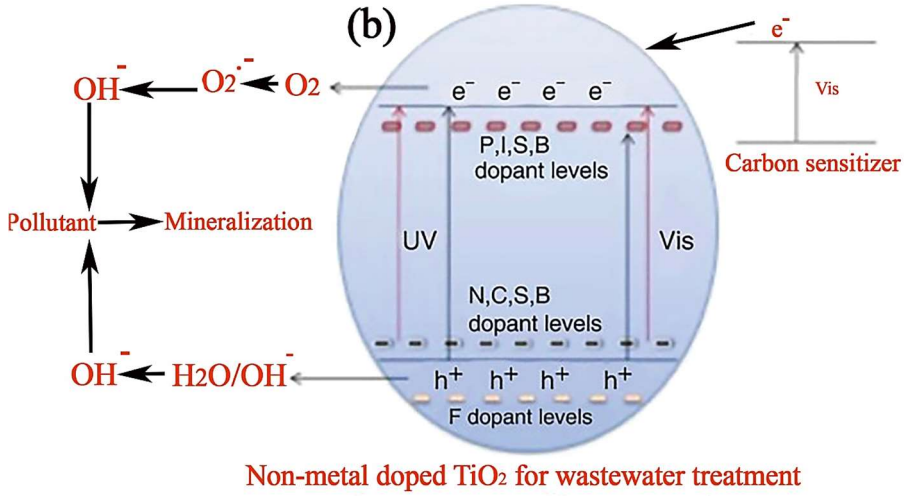

Figure 5. Photodegradation mechanism of contaminants by metals-doped (a) and non-metals-doped TiO_2 (b).

Numerous studies have been performed on the expansion of the solar absorption band by combining TiO_2 with new metals, intermediates and anions, which maximizes the performance of the photocatalyst [45]. Table 2 presents the influence of various metal dopants on the photocatalytic activity of TiO_2. Accordingly, Wang et al. (2019) synthesized 5% Pd-doped TiO_2 photocatalyst to degrade 2,2',4,4'-tetrabromodiphenyl ether from water under UV lamp and showed 100% photodegradation efficiency, which is a remarkable amount [70]. Also, Sescu et al. (2020) synthesized Au/TiO_2 photocatalyst using two different procedures such as incipient wet impregnation (IWI) and ultrasound impregnation (UI). Then, Au/TiO_2 (IWI) and Au/TiO_2 (UI) were used for degradation of 2,4 dinitrophenol under UV irradiation. According to their outcomes, the photodegradation efficiency of 2,4 dinitrophenol using Au/TiO_2 (IWI) and Au/TiO_2 (UI) were 50 and 37%, respectively, which were less than the photodegradation efficiency of pure TiO_2 (60%). Comparing these two methods displays that the IWI procedure is more efficient than the UI procedure. Therefore, they used the IWI procedure to synthesize Pd/TiO_2 for degradation of 2,4 dinitrophenol and Rhodamine 6G contaminants under UV irradiation. The photodegradation efficiency of 2,4 dinitrophenol and Rhodamine 6G using Pd/TiO_2 photocatalyst was 67% and 96%, respectively, indicating that the Pd/TiO_2 photocatalyst is able to remove Rhodamine 6G dye with a significant efficiency [72]. In another work, Yadav et al. (2020) utilized B-doped TiO_2 nanophotocatalyst for 4-nitrophenol removal from water. The utmost photodegradation efficiency using TiO_2 and B-doped TiO_2 was obtained 79 and 90%, respectively, indicating that the photodegradation efficiency of TiO_2 enhanced with its doping by boron [71]. In general, previous studies show that most photocatalytic processes are performed under UV light. Also, Ag and Pd dopants showed greater potential for photodegradation of organic contaminants than other dopants.

Table 2. Impact of various dopants on the TiO_2 photocatalytic activity.

Dopant	Light source/pollutant	Conditions	PE for TiO_2 (%)	PE for Doped TiO_2 (%)	Ref.
Ag	UV-A illumination/ 2,4,6-trichlorophenol	0.5 wt.% Ag, 120 min	-	95	[66]
Ag	Halogen lamp/MB	2 Wt.% Ag, 120 min	-	82.3	[67]

 doi:10.20944/preprints202406.0592.v1

Ni	Ultraviolet/Dipterex	pH 6, dipterex concentration= 40 mg/L, 2 h	-	83.5	[68]
Ce	UV lamp, crystal violet	0.8 mol Ce in TiO_2, 0.2 g/L catalyst, 30 ppm dye concentration, pH 6.5, intensity of 2000 W/cm^2	70	92	[15]
Fe	UV lamp/ Crystal violet	1.2 mol Fe in TiO_2, 0.2 g/L catalyst, 30 ppm dye concentration, pH 6.5, intensity of 2000 W/cm^2	70	80	[15]
Au	UV lamp/Total Organic Carbon	8.71 mg/L Total Organic Carbon, 15W UV lamp	-	93	[69]
Si	UV lamp/MB	20 h for TiO_2 and 2 h for Si-doped TiO_2, 10 ppm MB	68	86.7	[63]
Pd	UV lamp/2,2',4,4' -tetrabromodiphenyl ether	5% Pd, 300 WUV lamp	-	100	[70]
B	UV light/4-nitrophenol	5% B in TiO_2, 1 g/L catalyst dose, 1 mg/L 4-nitrophenol	79	90	[71]
Au/UI	UV irradiation/2,4 dinitrophenol	20 mg/L contaminant concentration, 120 min, 1 g/L catalyst dose	60	37	[72]
Au/IWI	UV irradiation/2,4 dinitrophenol	20 mg/L contaminant concentration, 120 min, 1 g/L catalyst dose	60	50	[72]
Pd/IWI	UV irradiation/2,4 dinitrophenol	20 mg/L contaminant concentration, 120 min, 1 g/L catalyst dose	60	67	[72]

 doi:10.20944/preprints202406.0592.v1

Pd/IWI	UV irradiation/ Rhodamine 6G	20 mg/L contaminant concentration, 120 min, 1 g/L catalyst dose	88	96	[72]

4. ZnO nano-photocatalyst

ZnO nanocatalyst is one of the most efficient catalysts in the degradation of organic contaminants due to its unique features like excellent oxidation ability, direct and extensive band gap in the spectral region close to UV, high photocatalytic activity, and high binding energy. UV light can be absorbed on ZnO at a wavelength lower than 385 nm [73]. Rock salt, wurtzite and cubic structure are important crystalline structures of ZnO. Among the 3 structures, the wurtzite structure of ZnO is the most common structure and has the utmost stability. Also, ZnO in the form of rock salt is wholly rare. At room temperature and pressure, the crystalline structure of ZnO is a hexagonal wurtzite. Moreover, ZnO can crystallize in the structure of wurtzite. The ZnO wurtzite structure is the most common form of ZnO due to its stability in environmental conditions [74]. Different structures of ZnO are exhibited in Figure 6. In the ZnO wurtzite structure, each Zn atom is surrounded by four O atoms. ZnO has many benefits compared to TiO_2, including low-cost, chemical stability, no toxicity, and abundance [75]. Other properties of ZnO include insoluble in water, odorless, and bitter taste. ZnO can be used in catalysis processes, fertilizers, rubber industry, paint industry, and cosmetics. The development of nano-ZnO with precisely controllable properties has recently gained considerable scientific attention [76].

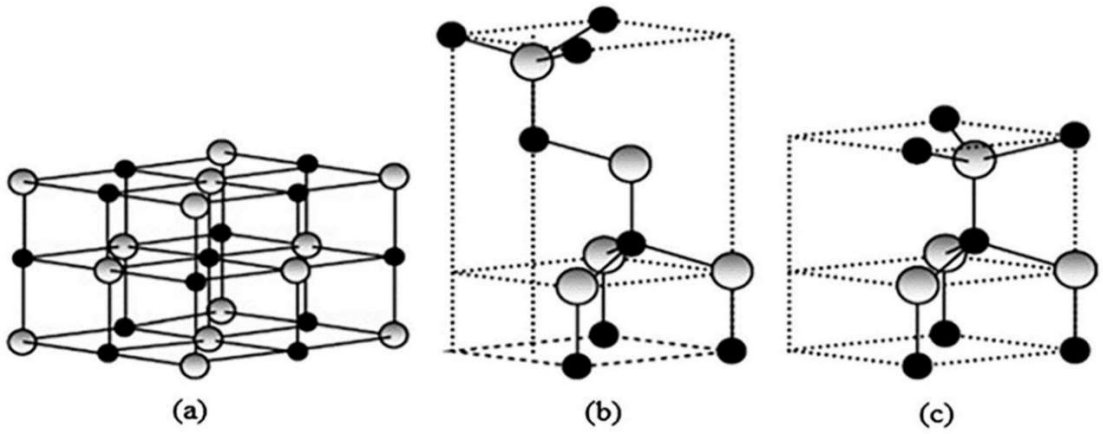

Figure 6. Different structures of ZnO, including salt rock (cubical structure) (a), zinc blend (cubical structure) (b), and wurtzite (hexagonal structure) (c) (Zn and O atoms are represented by grey and black spheres, respectively) [76].

Different zinc salts can be utilized to fabricate ZnO, including $Zn(C_2H_3O_2)_2.2H_2O$, $Zn(SO_4)_2.7H_2O$, $Zn(NO_3)_2{\cdot}6H_2O$, and $ZnCl_2$ [77]. ZnO nanoparticles and doped ZnO can be synthesized by various techniques, including pulsed-laser deposition, chemical coprecipitation, hydrothermal, thermal decomposition, sol-gel, liquid-solid solution, vapor condensation, microwave, and spray pyrolysis process [73,78]. Hydrothermal procedure is a well-known and efficient process for synthesizing ZnO nanoparticles, which is performed at high pressure and temperature [78]. Chemical coprecipitation is one of the most successful processes to synthesize ZnO nanoparticles with a fine particle size distribution. Chemical coprecipitation can prevent complex steps like alkoxide reflux and therefore takes less time than other methods [73]. Also, synthesizing ZnO nanoparticles by sol-gel and hydrothermal methods have several important advantages such as uniform particle distribution of particles and synthesis at low temperatures.

 doi:10.20944/preprints202406.0592.v1

However, microwave-based synthesis has attracted a lot of attention due to its advantages such as simpler, faster, and more energy efficient. The precursor solution is irradiated by the microwave source. Energy transfer via relaxation and/or resonance can lead to a relatively fast heating process. Also, heating process by the microwave source leads to uniform heating in a short time, which results in uniform distribution of particles [79].

4.1. Characterization of ZnO Nanocatalyst

ZnO nanocatalyst is a semiconductor with broad band-gap as well as high binding energy in environmental conditions. ZnO NPs have a better optical, electrical, and magnetic feature than ZnO microparticles. ZnO NPs also have unique physical, thermal, and chemical properties like biocompatibility, low cost, and non-toxic. ZnO is an environmentally friendly substance, which is well suited for a wide range of daily applications that pose no risk to human health. Also, ZnO NPs have longer shelf life compared to other metal oxides like Fe_2O_3, SiO_2, WO_3, and TiO_2. Because of its exceptional features, ZnO nanocatalyst can be utilized as a valuable catalyst to treat wastewater [77]. Owing to the band gap energy (3.2 eV) similar to ZnO with TiO_2, their photocatalytic capability is similar. Also, ZnO nanocatalyst is relatively cheaper than TiO_2 nanocatalyst, the use of ZnO is more economical in the large-scale water purification process. ZnO can adsorb a broad range of solar spectra and more optical quantum than many semiconductor metal oxides. However, the main disadvantage of ZnO is its wide band gap energy, therefore, the absorption of light by ZnO is limited to the visible light range. This leads to rapid recombination of light-generated charges, resulting in low photocatalytic performance [80]. The addition of doping affects the optical features of ZnO and possibly shifts the amplitude of optical absorption to the visible region. Therefore, the photocatalytic activity of ZnO can be enhanced by doping it with other materials, which is described in detail in Section 4.3 [72].

4.2. Photocatalysis Mechanism of ZnO

In a desirable photocatalytic reaction in the presence of zinc oxide particles and active oxidizing species like oxygen, organic contaminants can be converted to H_2O, CO_2, and inorganic acids. Photocatalytic reaction begins when ZnO NPs absorb photons from light with energies greater than their band gap energy. Thus, the photo-induced electron rises from the valence band to the conduction band, creating h^+ and e^- on the ZnO surface [81]. The presence of O atom as an electron absorber lengthens the pair of recombinant electron cavities and the formation of superoxide radicals. The reaction between h^+ and OH^- results in the production of hydroxyl radicals. Figure 7(a) indicates the photocatalytic mechanism of anionic- and cationic doped ZnO catalyst and photodegradation mechanism of the contaminant on the ZnO surface under sun light is illustrated in Figure 7(b) [82]. The reaction mechanism of ZnO in the photocatalytic process has several steps, which are presented below [83]:

$$ZnO + hv \rightarrow e^- + h^+$$

Absorbed oxygen: $O_2 + e^- \rightarrow O_2^{\cdot -}$

Water ionization: $H_2O \rightarrow OH^- + H^+$

Superoxide protonation: $O_2^{\cdot -} + H^+ \rightarrow HOO^{\cdot}$

$$HOO^{\cdot} + e^- \rightarrow HOO^-$$

$$HOO^- + H^+ \rightarrow H_2O_2$$

$$H_2O_2 + e^- \rightarrow OH^- + OH^{\cdot}$$

$$H_2O + h^+ \rightarrow H^+ + OH$$

Preprints.org (www.preprints.org) | NOT PEER-REVIEWED | Posted: 11 June 2024 doi:10.20944/preprints202406.0592.v1

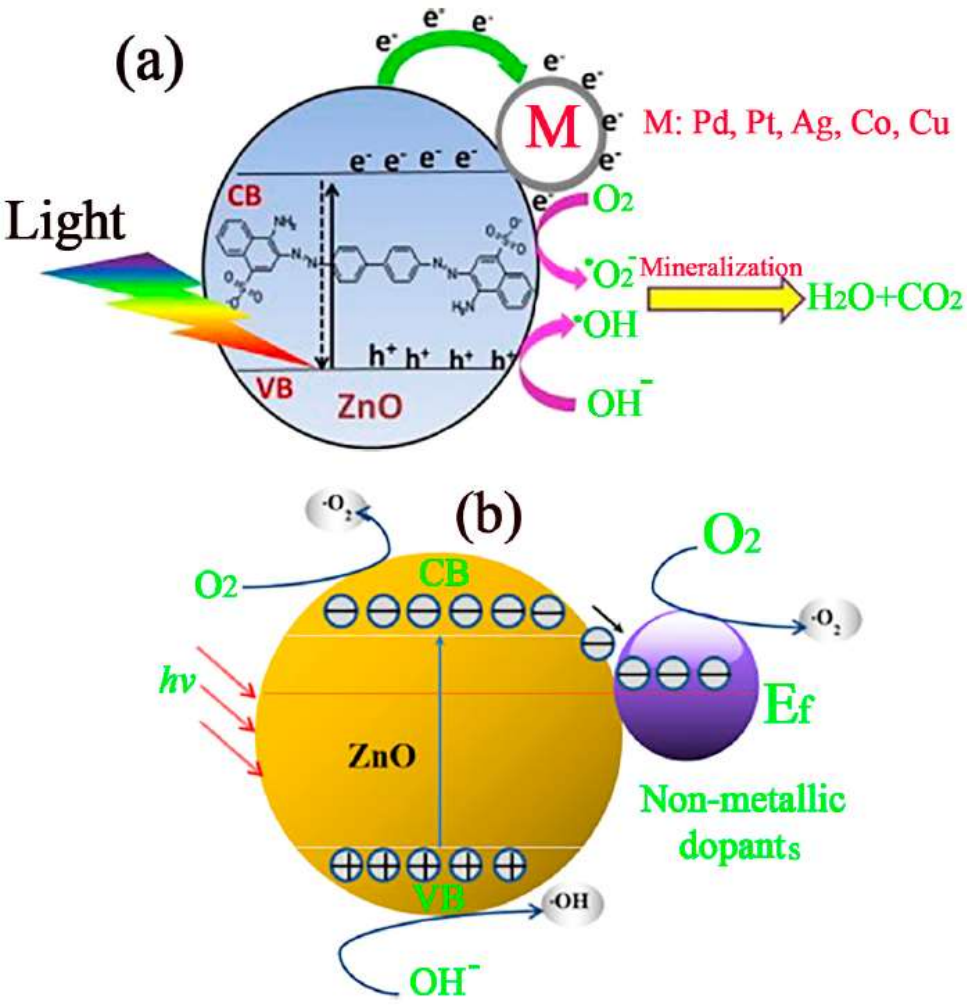

Figure 7. Catalytic mechanism by cationic and anionic dopants (a) and photodegradation mechanism under sun light (b) on the surface of ZnO NPs.

4.3. Improving the Photodegradation Efficiency of ZnO

The recombination of photo-produced h^+ and e^- is one of the main disadvantages of semiconductor photocatalysis. This recombination stage reduces quantum efficiency and wastes energy. Thus, the recombination process of e^-/h^+ must be inhibited to have an impressive photocatalysis process. Metal doping can counteract the recombination problem by increasing the isolation of charge between h^+ and e^-. Also, dopants can trap e^- and reduce the chance of electron/hole recombination, which inactivates the photocatalytic process. Moreover, the production of active oxygen species and hydroxyl radicals significantly increases the charge separation efficiency. In general, the dopant concentration, operating conditions, and the synthesis procedure have significant impacts on the metal-doped semiconductor photocatalysis process [84].

Anion-doped zinc oxide photocatalyst has shown higher photocatalytic degradation efficiency than pure zinc oxide. The presence of isolated N2p modes above the utmost ZnO valence band in the Ne ZnO sample increases its ability to absorb visible light. Under visible light irradiation, narrow-band gaps in N- ZnO require lower energy to induce the charge carriers (e^- and h^+). Increased photocatalytic activity of C-doped zinc oxide can be owing to many reasons, including increased adsorption of contaminants on the surface of catalyst, higher UV uptake than pure ZnO, creating new energy levels under the ZnO conduction band, where photoexcited e^- by these new energy levels are removed to avoid the electron hole from recombining. All these factors increase the number of charge carriers and improve the photodegradation performance. Also, the number of oxygen vacancies in ZnO have a key role in influencing the photo-activity of ZnO doped with S. In the photocatalytic reaction, oxygen vacancies become centers for trapping e^-. Therefore, the more the oxygen vacancies

Preprints.org (www.preprints.org) | NOT PEER-REVIEWED | Posted: 11 June 2024 doi:10.20944/preprints202406.0592.v1

there are, the greater the catalytic activity [85,86]. Figure 8 shows the mechanism of the pollutant degradation by metals and non-metals doped ZnO [87]. As shown in Figure 8(a), the metal doped on the ZnO surface contributes to generate e^- and subsequently O_2^- radicals, resulting in better photodegradation of organic contaminants. The same role is played by non-metals doped with ZnO to generate O_2^- radicals followed by the photodegradation of pollutants (Figure 8(b)).

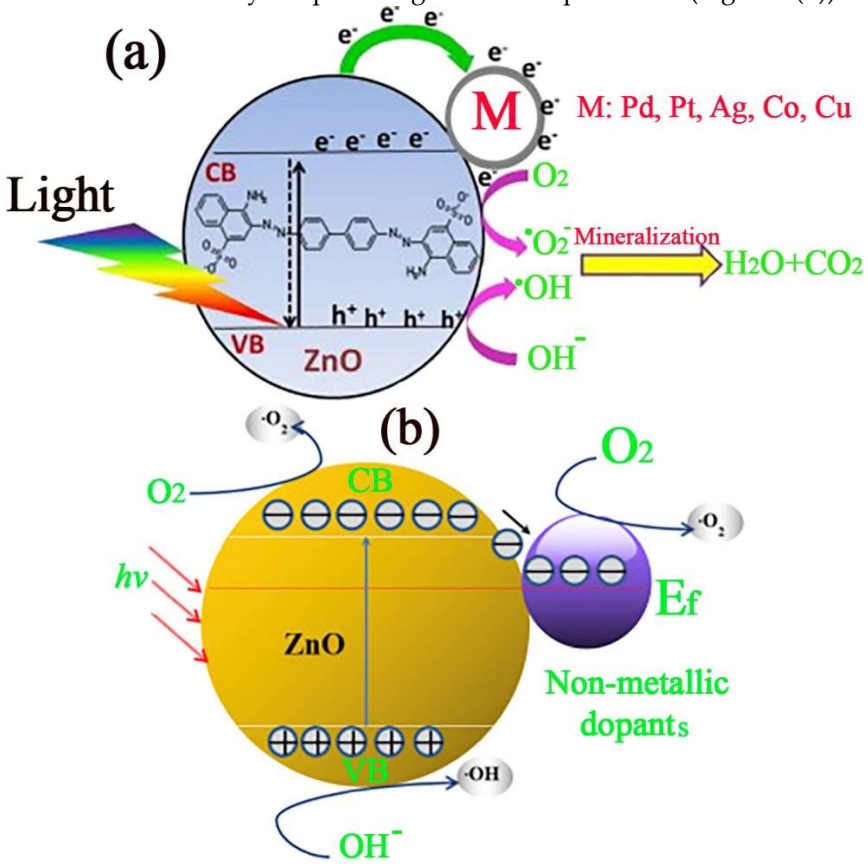

Figure 8. Photodegradation mechanism of contaminants using metals-doped ZnO (a) and non-metals doped ZnO (b).

Despite the high photodegradation efficiency of ZnO, studies show that the doped ZnO has a significant photocatalytic efficiency compared to the undoped ZnO. ZnO surface modification using cationic dopants has attracted much attention. The chemical, electrical, magnetic, and structural features of ZnO can be adjusted by adding cationic dopants such as Ni, Mn, Co, Al, and Sb. The doped elements are usually iso-morphic to Zn ion, like Cu(II), Co(II), Ni(II), and Mn(II). The doped ZnO photocatalyst shows a faster response to degradation of organic contaminants than pure ZnO [88]. Table 3 reports the impact of different metallic dopants on the photocatalytic efficiency of ZnO. As shown, Adeel and coworkers (2021) studied the degradation process of MO using Co-doped ZnO. The photodegradation efficiency of ZnO and Co-doped ZnO were 46 and 93%, showing that the photodegradation efficiency of ZnO doubled after its doping with Co [89]. In another work, Vallejo et al. (2020a) compared the photodegradation efficiency of MB using ZnO and Ag-doped ZnO. Their results displayed photodegradation efficiencies of 2.7 and 45.1% for ZnO and Ag-doped ZnO, respectively, indicating a remarkable increment in photodegradation efficiency after ZnO doping with Ag. These photodegradation efficiencies were attained after 120 min visible irradiation [90]. Also, Vallejo et al. (2020b) synthesized Co-doped ZnO and Cu-doped ZnO photocatalysts and compared their photodegradation efficiencies with ZnO in MB removal under visible light after 140 min. Their findings demonstrated that the photodegradation efficiencies of ZnO, Co-doped ZnO and Cu-doped ZnO were 2.7, 62.6, and 42.5%, respectively [91]. Moreover, Cr-doped ZnO was able to decompose MO dye with excellent photodegradation efficiency of 99.8% under UV-vis light

 doi:10.20944/preprints202406.0592.v1

illumination after 100 min [92]. Among these works, Cr-doped ZnO showed the highest photodegradation efficiency (99.8%) for removing methyl orange after 100 min under UV light.

Table 3. Comparing different metallic dopants in the ZnO structure on the photocatalytic activity.

Dopant	Light source/pollutant	Operating conditions	*PE (%) for ZnO	PE (%) for Doped ZnO	Ref.
Co	Visible light irradiation/MO	10 wt.% Co, 130 min, 100 mg/L MO	46	93	[89]
Ag	Visible irradiation/MB	5 wt.% Ag, 120 min	2.7	45.1	[90]
Co	Visible light irradiation/MB	5 wt.% Co, 10 ppm dye concentration, 140 min	2.7	62.6	[91]
Cu	Visible light irradiation/MB	5 wt.% Cu, 10 ppm dye concentration, 140 min	2.7	42.5	[91]
Cr	UV-vis light illumination/MO	1 wt.% Cr, 100 min	-	99.8	[92]
Sn	Sunlight/Brilliant green	120 min	72.6	96.52	[93]
Fe	Sunlight/MB	Time=3 h	90	95	[94]
Ta	Visible light irradiation/MB	20 min, 1 g/L catalyst dosage, pH 8, 10 mg/L dye concentration	-	97.5	[95]

*PE: Photodegradation efficiency.

Table 4 also reports the impact of various non-metallic dopants on the ZnO photocatalytic activity for some organic contaminants. As shown, Wu and coworkers (2014) studied the photodegradation performance of MB using N-doped ZnO under visible light irradiation and compared its results with pure ZnO. Their outcomes indicated that the photodegradation efficiency of MN using pure ZnO and N-doped ZnO photocatalysts are 76.2 and 81.6%, respectively [97]. Also, Li and coworkers (2012) used pure ZnO and C-doped ZnO for photodegradation of MB under visible light. After 60 min, C-doped ZnO was able to decompose MB with the photodegradation efficiency of 98.1%, which is a significant amount compared to pure ZnO (54.3%) [99]. Moreover, the photodegradation efficiency of Bisphenol A using C-doped ZnO under UV irradiation was 100%, indicating high degradation efficiency [101]. Furthermore, Fu et al. (2012) studied the photocatalytic reaction of MB dye using C-doped ZnO under visible light and compared the photodegradation efficiency of ZnO and C-doped ZnO. The highest photodegradation efficiency of ZnO and C-doped ZnO was achieved 26 and 80% under optimal conditions such as 2.5% catalyst and 200 ^{o}C, which showed a significant increase in the photodegradation efficiency after ZnO doping with C [100]. In general, most studies have performed by N- and C-doped ZnO photocatalysts and both dopants showed significant photodegradation activity. Therefore, these studies demonstrate that utilizing C- and N-doped ZnO photocatalysts is more attractive to researchers than other dopants.

 doi:10.20944/preprints202406.0592.v1

Table 4. Impact of various non-metallic dopants on the ZnO photocatalytic activity.

Dopant	Light source/pollutant	Conditions	PE (%) ZnO	PE (%) Doped ZnO	Ref.
N	UV light or Visible light irradiation/MB	-	-	99.6	[96]
N	Visible light irradiation/Rhodamine 6G	60 min, 0.01 g N	76.2	81.6	[97]
N	Visible light irradiation/Rhodamine B	10 mg/L dye concentration, Room temperature, 2 h	-	97	[98]
N	Visible light irradiation/MB	10 mg/L dye concentration, Room temperature, 2 h	-	99	[98]
C	Visible light/MB	60 min	54.3	98.1	[99]
C	Visible light/MB	2.5% Catalyst, 200 °C	26	80	[100]
C	UV irradiation/ Bisphenol A	24 h	-	100	[101]
C	Sunlight irradiation/ Rhodamine B	2.5 h	54.6	92.9	[102]

PE: Photodegradation efficiency.

5. Factors Affecting Photodegradation Efficiency

5.1. Photocatalyst Dosage

Catalyst dosage or catalyst loading is a critical factor on the photocatalytic efficiency of organic contaminants. Increasing the catalyst dose leads to an enhancement in the specific surface area of the catalyst, the creation of more active sites, and ultimately the formation of more hydroxyl and superoxide radicals. Thus, degradation of organic contaminants will be facilitated and a higher photodegradation efficiency will be attained. The photodegradation efficiency initially enhances by enhancing the photocatalyst dosage until it reached an optimal value. At the photocatalyst concentration beyond the optimal concentration, the photodegradation efficiency decreases because of light scattering. Increasing the photocatalyst dosage beyond the optimal value leads to the agglomeration of catalyst particles and then decrease the specific surface area of the catalyst to absorb light, which ultimately leads to a reduction in the degradation efficiency. On the other hand, it prevents light from penetrating into the sewage. As a critical result, an optimal value of catalyst must be determined to prevent overuse of the catalyst and to achieve maximum degradation efficiency [40].

In one study, Zhang and co-workers (2015) studied the photodegradation efficiency of MB using TiO_2 in the range of photocatalyst dosage from 1-10%. According to their outcomes, the maximum photodegradation efficiency of MB (93.78%) was attained at an optimal value of 7% [103]. Also, Notodarmojo et al. (2017) studied degradation efficiency of RB-5 dye from water and found that the degradation efficiency increases with increasing the TiO_2 photocatalyst concentration from 0.5 to 2.5 g/L. Therefore, 2.5 g/L was considered as the optimum photocatalyst dosage [104]. Moreover, Saiful Amran and co-workers (2019) investigated the maximum degradation efficiency of MB using carbon-doped TiO_2 in the photocatalyst dosage range of 1-3%. According to their outcomes, the highest photodegradation efficiency (82.67%) was obtained at 2 wt.% photocatalyst dosage [105]. Furthermore, Erdemoğlu et al. studied the influence of nano-TiO_2 dosage (0.1-1 wt.%) on photodegradation of CR under visible light. The nanocatalyst could remove 94% of CR at the catalyst dosage of 0.25 wt.%. By enhancing catalyst dosage from 0.25 to 1 wt.%, the photodegradation efficiency decreased [106].

5.2. Photocatalyst Structure

Photocatalytic efficiency is effectively influenced by the photocatalytic structure. The synthesis of nanostructured photocatalysts has recently received much attention because of their unique

 doi:10.20944/preprints202406.0592.v1

structures and features. There are various morphologies for nanostructured photocatalysts, including nanoflowers, nanosheets, nanowires, nanorods, nanodumbbells, nanobelts, and nanospiral disks. Some structures of these photocatalysts are illustrated in Figure 9. Nanostructured photocatalysts have a high specific active area with great catalytic strength. A high surface/volume proportion presents a better physical and chemical feature. Each of these structures has shown various photocatalytic features [107,108].

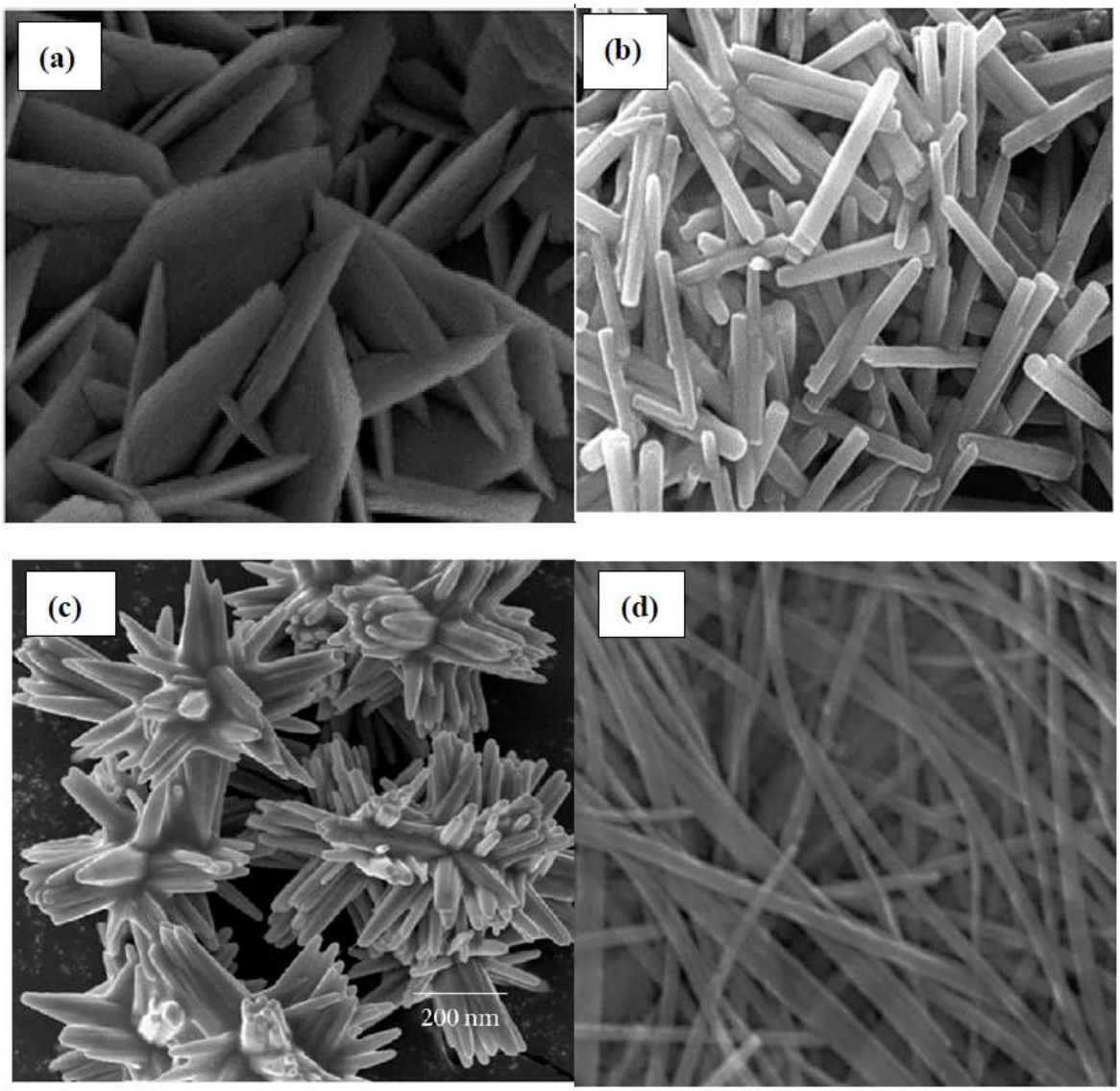

Figure 9. Different forms of ZnO nanostructured photocatalysts, including (a) nanosheets [109], (b) nanorods [110], (c) nanoflowers [111], and (d) nanowires [112].

5.3. Contaminant Concentration on Photodegradation Efficiency

Contaminant concentration has an important influence on the photocatalytic process. Previous studies show that the concentration of organic pollutant in aqueous solution has an undesirable impact on photodegradation efficiency. The higher the concentration of contaminants in the effluent, the lower the photodegradation efficiency, which is because the concentration of the target contaminant becomes more and more. Organic contaminants can be adsorbed on the photocatalyst surface. The number of contaminant molecules increases, while the number of active sites remains constant [113]. Hence, generating hydroxyl radicals are not enough and there will be only a few active sites on the photocatalyst surface to absorb hydroxyl ions. Consumption of hydroxyl radicals ($OH\cdot$) by the produced intermediates decreases the photodegradation efficiency in solutions with high

 doi:10.20944/preprints202406.0592.v1

contaminant concentration. Therefore, the lower the pollutant concentration, the less competition there is for consumption [114,115]. Parida and Parija (2006) investigated the impact of phenol concentration on the degradation efficiency using ZnO in various irradiation strength. Under solar irradiation, the photodegradation yield decreased from 100% to 60% with enhancing the phenol dosage, while under ultraviolet light, the photodegradation efficiency reduced from 94% to 52% with enhancing the phenol concentration [116]. Also, Benhabiles et al. (2016) studied the influence of MB dye concentration (10-30 mg/L) on the photocatalytic process by commercial TiO_2. After 5 h, 70% of MB dye was degraded by TiO_2 at MB concentration of 10 mg/L, while at MB concentration of 30 mg/L, the catalyst was able to remove only 30% of MB [117]. Moreover, Shelar et al. (2020) surveyed the impact of MB dye concentration (10-40 mg/L) on photodegradation using Ag-doped ZnO. The photodegradation efficiency reduced from 95% to 65% with enhancing MB dosage from 10 to 40 mg/L, indicating that the highest photodegradation efficiency occurs at the lowest dosage of MB dye [118].

Generally, previous studies demonstrate that the highest photodegradation efficiency of contaminants occurs at the lowest contaminant concentration.

5.4. pH

Solution pH plays a vital role in the photocatalytic reaction of water purification. pH can change the surface charge of the photocatalyst [119]. Determination of optimal pH in the photodegradation process depends on the zero-point charge (pH_{zpc}) of the photocatalyst. pH and the photodegradation rate do not have a specific relation. The TiO_2 photocatalyst will be negatively charged, if $pH > pH_{ZPC}$. In this case, TiO^- anion will be formed. Also, if $pH < pH_{ZPC}$, the TiO_2 photocatalyst will be positively charged and form $TiOH^+_2$ cation. Depending on the catalyst used, the surface charge of the photocatalyst at $4.5 < pH_{ZPC} < 7$ is neutral. When operating at pHzpc, the surface charge of TiO_2 photocatalyst is positively charged and absorbs negatively charged molecules electrostatically over time. Industrial effluents may be discharged at different pHs, which complicates the photocatalytic reaction. Also, hydroxyl radicals are rapidly eliminated at high pHs, inhibiting their reaction with the contaminant [40,115]. There are many effective factors on pH in the photocatalytic reaction, including electrostatic charge of catalyst particles, band structure, and crystals size. Each of these factors can alter the photocatalyst surface charge and generally alter the photodegradation efficiency [115]. Generally, the optimal pH in photodegradation depends on the contaminant and the photocatalyst. For example, Hameed et al. (2009) studied the impact of pH on the photodegradation efficiency of carbofuran using TiO_2/Ultraviolet and pH 7 was obtained as the optimal pH [120]. Also, Lopez-Alvarez et al. (2011) surveyed the impact of pH on the photodegradation efficiency of carbofuran using TiO_2/solar light and their outcomes showed that pH 7.6 is the best pH [121]. Moreover, in the work done by Saien and Khezrianjoo (2008) for degradation of carbendazim using TiO_2/Ultraviolet, the optimal pH was 4 [122]. Furthermore, Elmolla and Chaudhuri (2010) found the optimal pH of 11 for photodegradation of amoxicillin, ampicillin and claxocillin using ZnO/Ultraviolet [123]. In another work, the highest photodegradation efficiency of TiO_2 for MB removal was attained at pH of 11 [117]. Also, Shelar et al. studied the impact of pH on photodegrading MB dye in the range of 2-12 and found that the utmost photodegradaion efficiency is obtained at pH 8 [118].

5.5. Light Intensity and Wavelength

Photodegradation efficiency depends on the absorption of light by a catalyst [124]. Light intensity specifies how much light can be adsorbed by a photocatalyst at a given wavelength. The higher the light intensity, the more radiation is deposited on the photocatalyst surface, leading to the production of more hydroxyl radicals and enhances the reaction rate. At higher light intensities, the photodegradation reaction depends on the mass transfer between the reactants, because the photocatalyst surface is completely covered by saturated solids, limiting the mass transfer for sorption and desorption. Therefore, the photocatalytic reaction speed remains constant in spite of an increase in the intensity of light. Previous studies have shown that there is a relationship between the

 doi:10.20944/preprints202406.0592.v1

photodegradation efficiency of the contaminant and light intensity for different organic compounds. The generation of hydroxyl radicals increases with increasing light intensity, which leads to an improvement in the degradation rate [115,125]. Elaziouti et al. investigated the impact of light intensity in the range of 50-90 j/cm^2 on the photodegradation efficiency of CR and benzopurpurine 4B. The photodegradation efficiency of CR and benzopurpurine 4B increased with enhancing the light intensity from 50 to 80 j/cm^2 and 50 to 90 j/cm^2, respectively. Because more photons at higher light intensities will be available for excitation on the catalyst surface and more electron-hole pairs can be produced [126].

Based on the wavelength of UV irradiation, there are three electromagnetic spectra, including UV-A, UV-B and UV-C. These are categorized based on the wavelength range. For example, the light wavelength range for UV-C, UV-B, and UV-A is between 100-280, 280-315, and 314-400 nm, respectively [127]. Because of the shorter penetration of higher energy photons, the photodegradation rate is greater at 254 nm, which increases the number of pairs of electron holes produced to decompose the target contaminant [128].

5.6. Temperature

It is better to perform the photodegradation reaction at 25 ^{o}C and 1 bar because of photonic activation, which is useful to purify water, by which the heating stage can be eliminated to save energy. However, the optimum temperature for photocatalytic reaction can occur at 20-80 °C. The results show that the photodegradation efficiency of organic pollutants increases with enhancing the reaction temperature, however, it may decline the adsorption capacity of reactive species and dissolved oxygen, leading to lower photodegradation efficiency [129]. Chen and coworkers studied the impact of temperature (0-50 ^{o}C) on the photocatalytic activity of TiO_2 and Pd/TiO_2 photocatalysts for MB elimination under UV light, and their outcomes demonstrated that the photodegradation efficiency increases with raising temperature [130]. Also, Hu and coworkers investigated the impact of temperature on photodegradation of MO dye using TiO_2. According to their results, under UV-vis irradiation, the photocatalytic activity of TiO_2 increased by enhancing temperature from 38 to 100 ^{o}C. Hence, the reaction was endothermic. Also, the reaction rate constant increased from 0.00031 to 0.00217 min^{-1} with enhancing temperature from 34 to 100 ^{o}C, respectively [131]. Moreover, Barakat and coworkers studied the influence of temperature (5-55 ^{o}C) for degradation of rhodamine B using Ag-doped TiO_2. The highest photodegradation efficiency under irradiation occurred at 55 ^{o}C [132]. Generally, the photodegradation efficiency of organic contaminants increases with enhancing temperature and the highest removal performance occurs at high temperatures.

5.7. Reaction Time

Irradiation time or reaction time is a critical factor in the photodegradation process and is when the contaminant is exposed to light or photon energy. Many researches have investigated the impact of reaction time on the photodegradation efficiency of organic contaminants using TiO_2 and ZnO photocatalysts. The longer the reaction time, the higher the photodegradation efficiency of the contaminant [40]. According to the work done by Shi et al. (2019), eliminating MO using TiO_2/chitosan increased with enhancing the reaction time and finally reaches equilibrium. At the beginning of the photocatalytic reaction, there is a large number of active sites at the photocatalyst surface to attach with MO molecules, resulting in a high degradation efficiency. After the equilibrium reaction time, no change in the photodegradation efficiency was observed [133]. Elaziouti et al. studied the impact of reaction time (0-80 min) on the photodegradation efficiency of CR and benzopurpurine 4B. 95% of CR dye and 97.2% of benzopurpurine 4B were degrade using 1 g/L ZnO after 60 and 80 min, respectively [126]. Also, Erdemoğlu et al. studied the influence of irradiation time on photodegradation of CR dye using TiO_2. Under visible irradiation, CR was completely decomposed after 30 min [106].

 doi:10.20944/preprints202406.0592.v1

6. Recyclability of ZnO and TiO_2 Photocatalysts

The most important factor for the practical application of catalyst is its recyclability and stability. Catalyst recyclability shows how many times a catalyst can be utilized in the catalytic process. After repeated reuse, the degradation efficiency of the catalyst is reduced, which may be due to saturating active sites, inactivating active sites, and chemical decomposition of the catalyst structure. If the degradation efficiency changes slightly after repeated use of the catalyst, it indicates that the catalyst is highly reusable. Thus, determining the reusability of a catalyst is critical [18,134]. Table 5 reports the reusability of various composites of ZnO and TiO2 in different cycles.

Table 5. Stability and recyclability of various composites of ZnO and TiO_2.

Catalyst	Pollutant	PE* (%)	PE (%)after n cycles	Ref.
ZnO nanorodes	imidazole	83%	n=4, 80%	[135]
Ag-doped ZnO nanocomposite	MB	95%	n=4, 89.5%	[118]
Fe_3O_4@S-doped ZnO	ofloxacin	Above 90%	n=6, Above 90%	[136]
ZnO NPs	MB	93.25%	n=5, 86.63%	[22]
ZnO NPs	Rhodamine B	91.06%	n=5, 83.61%	[22]
Mg-doped ZnO nanorodes	MB and ciprofloxacin	82%	n=4, 75%	[137]
2%Au-doped TiO_2 nanocatalyst	MO	100%	n=11, 100%	[138]
Sm/N co-doped TiO_2/diatomite	tetracycline	87.1%	n=5, 83.2%	[139]
C-doped TiO_2/carbon nanofibrous	rhodamine B	94.2%	n=6, 92%	[140]
TiO_2	MO	58.3%	n=10, 36.1%	[141]
TiO_2/polyaniline	MO	86%	n=10, 46.2%	[141]
Fe_3O_4/AC/TiO_2	MB	98%	n=7, 93%	[142]
2-(methacryloyloxy) ethyltrimethylammonium chloride/TiO_2	MB	99.66%	n=20, 98.7%	[143]
TiO_2/2NiO	MB	100%	N=5, 72.6%	[134]

*PE: Photodegradation efficiency.

Nikoofar et al. (2015) synthesized ZnO nanorodes for imidazole removal. They studied the reusability of ZnO nanorodes in 4 runs and their results showed that the elimination efficiencies of imidazole after the first, second, third and fourth cycles were 83%, 83%, 81% and 80%, respectively, which indicates that the elimination efficiency has declined slightly (less than 3% after 4 reuse cycles), showing remarkable reusability of ZnO nanorodes [135]. In another study, the reusability of Ag/ZnO nanocomposite was studied in eliminating MB, MO and CR in 5 successive steps. A slight decrease in dye removal efficiency was observed after 5 cycles, indicating significant recyclability of Ag/ZnO for eliminating organic dyes [144]. Also, Shelar et al. (2020) investigated the stability and recyclability of Ag-doped ZnO nanocatalyst for eliminating MB dye. The photodegradation efficiency of MB was 95%. Then, the nanocatalyst was eluted 3 times with deionized water and reused in the photocatalytic process. After 4 cycles, the photodegradation efficiency reduced to 89.5%, indicating high stability of Ag-doped ZnO nanocatalyst [118]. Moreover, Fe_3O_4@S-doped ZnO was utilized for degrading ofloxacin. The recyclability study illustrated that the photodegradation efficiency of ofloxacin was

 doi:10.20944/preprints202406.0592.v1

above 90% after 6 cycles, indicating remarkable stability and reusability of Fe_3O_4@S-doped ZnO [136]. Furthermore, Khan and coworkers (2021) studied the reusability of ZnO NPs for photodegradation of MB and Rhodamine B dyes after 5 consecutive cycles. The photodegradation efficiencies of MB and Rhodamine B dyes were decreased from 93.25 to 86.63% and 91.06 to 83.61% after 5 cycles, respectively, indicating that the efficiency reduction percentage is less than 10%. ZnO indicates excellent photocatalytic activity and high stability after 5 cycles [18]. Besides, Ikram et al. (2021) studied the reusability of Mg-doped ZnO nanorods for eliminating a mixture of MB and ciprofloxacin. After 4 cycles, the photodegradation efficiency slightly reduced from 82 to 75% after 40 min [137].

Also, Padikkaparambil and coworkers (2013) studied the reusability of 2%Au-doped TiO_2 nanocatalyst for MO photodegradation under UV irradiation in 11 reuse cycles. Under operating conditions (3 g/L catalyst, 10 mg/L MO and 1 h irradiation time), the photocatalytic activity of Au/TiO_2 did not change (about 100% photodegradation efficiency) even after 10 consecutive tests, which indicates the high reusability of 2%Au-TiO_2 [138]. Also, Wu and Zhang (2019) studied the reusability and stability of Samarium/Nitrogen co-doped TiO_2/diatomite for eliminating tetracycline under visible light. After 5 cycles, the photodegradation efficiency reduced from 87.1% to 83.2% (less than 5% reduction), indicating high stability and significant reusability of the Samarium/Nitrogen co-doped TiO_2/diatomite catalyst [139]. Moreover, Song et al. studied the reusability of C-doped TiO_2/carbon nanofibrous in removing rhodamine B. The nanocatalyst showed the photodegradation efficiency of 94.2% under UV light. After six reusing cycles, the photodegradation efficiency reached to 92%, showing significant reusability and stability of C-doped TiO_2/carbon nanofibrous [140]. In another work, Bahrudin and coworkers (2019) studied the reusability of TiO_2 and TiO_2/polyaniline for MO dye photodegradation. After ten reuse cycles, the photodegradation efficiency of MO using TiO_2 and TiO_2/polyaniline decreased from 58.3 to 36.1% and 86 to 46.2%, respectively [141]. Moreover, Moosavi et al. (2020) studied the recyclability and stability of Fe_3O_4/AC/TiO_2 for 7 cycles of MB photodegradation. After 7 reuse cycles, the photodegradation efficiency reduced from 98 to 93% (about 5% reduction). They attributed the decrease in the photodegradation efficiency after 7 cycles to the following reasons: i) Particles losses may take place in washing and drying steps, which result in lower doses in the next cycle, leading to the decrease in the surface catalytic activity as well as the efficiency. ii) Characteristics of the catalyst like aggregation may change during different cycles, because aggregation of particles reduces the specific surface area as well as number of active sites. iii) The catalytic activity of the catalyst dwindles after each cycle due to blockage of active sites and pores [142]. Furthermore, the reusability of 2-(methacryloyloxy) ethyltrimethylammonium chloride/TiO_2 photocatalyst was studied for MB removal under UV irradiation. The photodegradation efficiency of the aforementioned photocatalyst after 270 min was 99.66% and after 20 reuse cycles, the photodegradation efficiency reached 98.7%, i.e., a reduction of less than 1% in the photodegradation efficiency, indicating remarkable stability of the photocatalyst [143]. Besides, TiO_2/2NiO photocatalyst was used to decompose MB in 5 reuse cycles and the outcomes showed that the photodegradation efficiency of MB using TiO_2/2NiO reduced from 100% to 72.6% after 5 cycles, indicating its high stability [134].

In general, examining the reusability of ZnO and TiO_2 nanocatalysts demonstrates that they have high reusability and their utilization in industrial applications is cost-effective. Also, adding metallic and non-metallic dopants to the structure of TiO_2 and ZnO catalyst increased their stability.

7. Literature Review

So far, many works have been done on the removal of organic compounds by catalysts. Most of these catalysts are based on TiO_2 or ZnO, because these catalysts have shown high performance compared to other catalysts. These catalysts are able to degrade organic contaminants in the presence of light or UV. For example, TiO_2 was able to eliminate phenol, nitrobenzene and MO with degradation efficiencies of 100%. But the degradation efficiency of toluene by TiO_2 photocatalyst was 71% [145]. Also, Razip and coworkers (2019) synthesized Fe_3O_4/TiO_2 nanocatalyst and used it in the removal of MO from wastewater. After 1h UV irradiation, the photodegradation efficiency of MO

 doi:10.20944/preprints202406.0592.v1

dye was obtained 90.3% [22]. In another study, Nagaraju et al. (2020) investigated the photocatalytic degradation of chlorobenzene from water using several catalysts such as ZnO, Pb/ZnO, Cd/ZnO and Ag/ZnO in the presence of LED light and tungsten light. Among these photocatalysts, Pb/ZnO was able to decompose chlorobenzene with 100% degradation efficiency in the presence of both lights. Also, pure ZnO showed the minimum degradation efficiency (71%) in the presence of LED light [28]. Also, carbon-doped TiO_2 nanocatalyst was able to eliminate methyl ethyl ketone under UV light with a photodegradation efficiency of 94% [23]. $Bi_{12}TiO_{20}$ nanophotocatalyst could remove cefixime with a degradation efficiency of 94.93% after 3 h, while $Bi_{12}ZnO_{20}$ removed 80% of cefuroxime from water after 4 h [146]. Moreover, Akhlaghian and Najafi (2018) synthesized $CuO/WO_3/TiO_2$ nanocatalyst for eliminating 4-Chlorophen. According to their outcomes, the aforementioned nanocatalyst was able to remove the pollutant with a degradation efficiency of 94.8%, which was obtained in the catalyst dosage of 0.75 g/L and H_2O_2 amount of 563.16 mmol/L, after 3 h [21]. Furthermore, Elmolla and Chaudhuri (2010) utilized ZnO nanophotocatalyst for removing Amoxicillin, Ampicillin, and Claxocillin and their outcomes demonstrated that ZnO could eliminate all contaminants with significant photodegradation percentage of 100% under ultraviolet after 180 min [123]. Table 6 reports the performance of TiO_2 and ZnO nanocatalysts in photodegradation of organic contaminants.

Table 6. The performance of TiO_2 and ZnO nanocatalysts and their derivatives in degrading different organic pollutants.

Nanocatalysts	Contaminants	Optimal conditions	DE (%)	References
TiO_2	Nitrobenzene	* CD=O.1M, CC=50 ppm	100	[145]
TiO_2	Parathion	CD=1 g/L, CC=50 ppm	70	[147]
TiO_2	Toluene	CD=5 g, CC=45 ppm	71	[145]
TiO_2	Phenol	1.8 g/L catalyst dose	100	[145]
TiO_2	Benzene	CD=5 g, CC=45 ppm	72	[148]
TiO_2	MO	CD=3 g/L, CC=30 ppm	100	[145]
Fe_3O_4/TiO_2 (P25)	MO	1 h under UV light irradiation	90.3	[22]
Fe_3O_4/TiO_2 (UV100)	MO	1 h under UV light irradiation	51.6	[22]
$CuO/WO_3/TiO_2$	4-Chlorophen	CD= 0.75 g/L, H_2O_2 amount=563.16 mmol/L, 3 h	94.8	[21]
$CuO/WO_3/TiO_2$	3-Phenyl-1-propan	CD= 0.75 g/L, H_2O_2 amount=563.16 mmol/L, 3 h	85.13	[21]
Carbon-doped TiO_2	Methyl ethyl ketone	Under UV light	94	[23]
La/TiO_2	Ramazol Brilliant Blue	-	72	[22]
PVP/TiO_2/polydopamine	malachite green	60 min, 10 mg/L of dye	45	[149]

 doi:10.20944/preprints202406.0592.v1

PVP/TiO_2/polydopamine	MB	60 min, 10 mg/L of dye	25	[149]
PVP/TiO_2/polydopamine	MO	60 min, 10 mg/L of dye	24	[149]
ZnO	Amoxicillin	Ultraviolet, pH=11, Catalyst dose=0.5 g/L, time 180 min	100	[123]
ZnO	Ampicillin	Ultraviolet, pH=11, Catalyst dose=0.5 g/L, time 180 min	100	[123]
ZnO	Claxocillin	Ultraviolet, pH=11, Catalyst dose=0.5 g/L, time 180 min	100	[123]
rGO/Fe_3O_4/ZnO	MV	120 min, CD= 0.04 g/L	83.5	[26]
Fe_3O_4/CuO/ZnO/graphene	MB	120 min, CD= 0.3 g/L	93	[25]
Tungsten/silver/ZnO	Ponceau 4R	pH 5.64, CD= 0.08 g/L, 25°C	78.8	[27]
$Bi_{12}TiO_{20}$	Cefixime	3 h	94.93	[146]
$Bi_{12}ZnO_{20}$	Cefuroxime	4 h	80	[29]
$ZnBi_2O_4$	Cefixime	Solar light (98 mW/cm^2), 30 min	89	[150]
$ZnBi_2O_4$	Cefixime	UV irradiation (20 mW/cm^2), 2h	88	[150]
Ag/TiO_2	Phenol	pH 7, CD= 1.5 g/L, CC= 5 ppm, power light= 18 W	82.65	[151]
ZnO/SnO_2	MB	pH 12, CD= 0.5 g/L, time 60 min	96	[152]
Pure ZnO	Chlorobenzene	LED light	71	[28]
Pb/ZnO	Chlorobenzene	LED light	100	[28]
Ag/ZnO	Chlorobenzene	LED light	95	[28]
Cd/ZnO	Chlorobenzene	LED light	90	[28]
Pure ZnO	Chlorobenzene	Tungsten light	90	[28]
Pb/ZnO	Chlorobenzene	Tungsten light	100	[28]
Ag/ZnO	Chlorobenzene	Tungsten light	83	[28]
Cd/ZnO	Chlorobenzene	Tungsten light	73	[28]

*CC=Contaminant concentration; CD=catalyst dose.

 doi:10.20944/preprints202406.0592.v1

8. Conclusion and Future Perspectives

TiO_2 and ZnO photocatalysts under either UV light or solar irradiation were studied for degradation of organic compounds from wastewater. These catalysts have outstanding features like low cost, excellent degradation efficiency, high photocatalytic activity, etc. and are known as important catalysts in the water and wastewater industry. Both catalysts have been shown to be usable in the presence of sunlight and UV light, but the results generally indicate that using UV light is more efficient. Previous studies have shown that a mix of these catalysts with other materials can enhance the degradation efficiency of organic compounds. In this review study, the impact of various factors like temperature, time, photocatalyst loading, photocatalyst shape, pH, light wavelength and light intensity was investigated on degrading organic compounds and the outcomes demonstrated that pH, photocatalyst dosage, temperature and light intensity have significant impact on the photodegradation efficiency. Also, impacts of these photocatalysts on the degradation rate of various organic compounds from wastewater were fully surveyed. Moreover, various dopants can be utilized in the structure of TiO_2 and ZnO nanocatalysts, so the impact of adding metal and non-metal dopants on their structures were fully studied. Studies show that the addition of some metal dopants such as Ag, Pd, and Co and non-metal dopants such as C- and N- in the structure of ZnO and TiO_2 significantly increases the photodegradation performance of organic contaminants. Furthermore, the reusability of ZnO and TiO_2 catalysts cleared that they have high stability and significant reusability. Therefore, they can be used in several cycles without significant decrease in their photocatalytic activity. 2%Au-doped TiO_2 nanocatalyst with a photodegradation efficiency of 100% after 11 reuse cycles showed outstanding stability for elimination of methyl orange dye. Also, the photodegradation efficiency of 2-(methacryloyloxy) ethyltrimethylammonium chloride/TiO_2 photocatalyst reduced from 99.66% to 98.7% after 20 reuse cycles for elimination of MB dye, indicating remarkable stability.

Generally, previous studies have shown that they can remove more than 90% of most organic contaminants. Therefore, both metals and non-metals doped TiO_2 and ZnO are strongly recommended for elimination of organic compounds from municipal and industrial wastewaters.

Funding: This research was funded by the Deanship of Scientific Research at King Khalid University under grant number RGP.2/367/45.

Data Availability Statement: Data are contained within the article.

Acknowledgments: The authors extend their appreciation to the Deanship of Scientific Research at King Khalid University for funding this work through the Large Group Project under grant number RGP.2/367/45.

Conflicts of Interest: The authors declare no conflicts of interest.

References

1. Tamjidi, S.; Moghadas, B.K.; Esmaeili, H.; Khoo, F.S.; Gholami, G.; Ghasemi, M. Improving the surface properties of adsorbents by surfactants and their role in the removal of toxic metals from wastewater: A review study. *Process Saf. Environ. Prot*. **2021**, *148*, 775-795.
2. Yang, Y. Dynamic Relationship of Urban and Rural Water Shortage Risks Based on the Economy–Society–Environment Perspective. *Agriculture* **2022**, *12*, 148.
3. Yao, L.; Selmi, A.; Esmaeili, H. A review study on new aspects of biodemulsifiers: Production, features and their application in wastewater treatment. *Chemosphere* **2021**, *284*, 131364.
4. Khaleghi, H.; Esmaeili, H.; Jaafarzadeh, N. B. Ramavandi, Date seed activated carbon decorated with CaO and Fe3O4 nanoparticles as a reusable sorbent for removal of formaldehyde. *Korean J. Chem. Eng*. **2022**, *39*, 146-160.
5. Esmaeili, H.; Esmaeilzadeh, F.; Mowla, D. Effect of surfactant on stability and size distribution of gas condensate droplets in water. *J. Chem. Eng. Data* **2014**, *59*, 1461-1467.
6. Kuhad, R.C.; Gupta, R. Biological remediation of petroleum contaminants. In Advances in applied bioremediation, Springer, Berlin, Heidelberg **2009**, 173-187.
7. Lürling, M.; Kang, L.; Mucci, M.; van Oosterhout, F.; Noyma, N.P.; Miranda, M.; Huszar, V.L.; Waajen, G.; Marinho, M.M. Coagulation and precipitation of cyanobacterial blooms. *Ecol. Eng.* **2020**, *158*, 106032.
8. Kumar, V.; Othman, N.; Asharuddin, S. Applications of natural coagulants to treat wastewater− a review. *MATEC Web of Conferences*. *EDP Sciences* **2017**, *103*, 06016.

9. Sugita, T. Study of Water Treatment Using Photocatalytic Material. Doctoral dissertation, Gunma University, **2015**.
10. Karale, R.S.; Wadkar, D.V.; Wagh, M.P. Effect of hydrogen peroxide and ferrous ion on the degradation of 2-Aminopyridine. *J. Appl. Water Eng. Res*. **2023**, *11*, 54-65.
11. Liang, H.; Esmaeili, H. Application of nanomaterials for demulsification of oily wastewater: A review study. *Environ. Technol. Innov.* **2021**, *22*, 101498.
12. Cuerda-Correa, E.M.; Alexandre-Franco, M.F.; Fernández-González, C. Advanced oxidation processes for the removal of antibiotics from water. An overview. *Water* **2020**, *12*, 102.
13. Rawal, J.; Kamran, U.; Park, M.; Pant, B.; Park, S.J. Nitrogen and Sulfur Co-Doped Graphene Quantum Dots Anchored TiO2 Nanocomposites for Enhanced Photocatalytic Activity. *Catalysts* **2022**, *12*, 548.
14. Xie, Y.; Hu, J.; Esmaeili, H.; Wang, D.; Zhou, Y. A review study on wastewater decontamination using nanotechnology: Performance, mechanism and environmental impacts. *Powder Technol.* **2022**, *412*, 118023.
15. Shirsath, S.R.; Pinjari, D.V.; Gogate, P.R.; Sonawane, S.H.; Pandit, A.B. Ultrasound assisted synthesis of doped TiO2 nano-particles: characterization and comparison of effectiveness for photocatalytic oxidation of dyestuff effluent. *Ultrason. Sonochem.* **2013**, *20*, 277-286.
16. Esmaeili, H. A critical review on the economic aspects and life cycle assessment of biodiesel production using heterogeneous nanocatalysts. *Fuel Process. Technol.* **2022**, *230*, 107224.
17. Hu, M.; Yao, Z.; Wang, X. Characterization techniques for graphene-based materials in catalysis. *AIMS Mater. Sci.* **2017**, *4*, 755-788.
18. Khan, M.; Ware, P.; Shimpi, N. Synthesis of ZnO nanoparticles using peels of Passiflora foetida and study of its activity as an efficient catalyst for the degradation of hazardous organic dye. *SN Appl. Sci.* **2021**, *3*, 1-17.
19. Bruno, M.E.; Tasat, D.R.; Ramos, E.; Paparella, M.L.; Evelson, P.; Rebagliati, R.J.; Cabrini, R.L.; Guglielmotti, M.B.; Olmedo, D.G. Impact through time of different sized titanium dioxide particles on biochemical and histopathological parameters. *J. Biomed. Mater. Res. A.* **2014**, *102*, 1439-1448.
20. Yu, C.; Cai, D.; Yang, K.; Yu, J.C.; Zhou, Y.; Fan, C. Sol–gel derived S,I-codoped mesoporous TiO2 photocatalyst with high visible-Light photocatalytic activity. *J. Phys. Chem. Solids* **2010**, *71*, 1337–1343.
21. Akhlaghian, F.; Najafi, A. CuO/WO3/TiO2 photocatalyst for degradation of phenol wastewater. *Sci. Iran.* **2018**, *25*, 3345-3353.
22. Razip, N.I.M.; Lee, K.M.; Lai, C.W.; Ong, B.H. Recoverability of Fe3O4/TiO2 nanocatalyst in methyl orange degradation. *Mater. Res. Express* **2019**, *6*, 075517.
23. Shayegan, Z.; Haghighat, F.; Lee, C.S. Carbon-doped TiO2 film to enhance visible and UV light photocatalytic degradation of indoor environment volatile organic compounds. *J. Environ. Chem. Eng.* **2020**, *8*, 104162.
24. Bai, L.; Liu, L.; Pang, J.; Chen, Z.; Wei, M.; Wu, Y.; Dong, G.; Zhang, J.; Shan, D.; Wang, B. N,P-codoped carbon quantum dots-decorated TiO_2 nanowires as nanosized heterojunction photocatalyst with improved photocatalytic performance for methyl blue degradation. *Environ. Sci. Pollut. Res.* **2022**, *29*, 9932–9943.
25. Tju, H.; Taufik, A.; Saleh, R. Enhanced UV photocatalytic performance of magnetic Fe3O4/CuO/ZnO/NGP nanocomposites. *J. Phys. Conf. Ser.* **2016**, *710*, 012005.
26. Thangavel, S.; Thangavel, S.; Raghavan, N.; Krishnamoorthy, K.; Venugopal, G. Visible-light driven photocatalytic degradation of methylene-violet by rGO/Fe3O4/ZnO ternary nanohybrid structures. *J. Alloys Compd.* **2016**, *665*, 107–112.
27. Vafaee, M.; Olya, M.E.; Drean, J.Y.; Hekmati, A.H. Synthesize, characterization and application of ZnO/W/Ag as a new nanophotocatalyst for dye removal of textile wastewater; kinetic and economic studies. *J. Taiwan. Inst. Chem. Eng*. **2017**, *80*, 379-390.
28. Nagaraju, P.; Puttaiah, S.H.; Wantala, K.; Shahmoradi, B. Preparation of modified ZnO nanoparticles for photocatalytic degradation of chlorobenzene. *Appl. Water Sci.* **2020**, *10*, 1-15.
29. Baaloudj, O.; Nasrallah, N.; Assadi, A.A. Facile synthesis, structural and optical characterizations of Bi12ZnO20 sillenite crystals: Application for Cefuroxime removal from wastewater. *Mater. Lett*. **2021**, *304*, 130658.
30. Liu, Q.; Zhao, Z.; Li, H.; Su, M.; Liang, S.X. Occurrence and removal of organic pollutants by a combined analysis using GC-MS with spectral analysis and acute toxicity. *Ecotoxicol. Environ. Saf.* **2021**, *207*, 111237.
31. Jain, M.; Khan, S.A.; Sharma, K.; Jadhao, P.R.; Pant, K.K.; Ziora, Z.M.; Blaskovich, M.A. Current perspective of innovative strategies for bioremediation of organic pollutants from wastewater. *Bioresour. Technol.* **2022**, *344*, 126305.
32. Aguirre Hernandez, E.A. Management of Produced Water from the Oil and Gas Industry: Characterization, Treatment, Disposal and Beneficial Reuse. Doctoral dissertation, Politecnico di Torino. 2021.
33. David, E.; Niculescu, V.C. Volatile Organic Compounds (VOCs) as Environmental Pollutants: Occurrence and Mitigation Using Nanomaterials. *Int. J. Environ. Res. Public. Health.* **2021**, *18*, 13147.

 doi:10.20944/preprints202406.0592.v1

34. Ramirez Castillo, F.Y.; Avelar González, F.J.; Garneau, P.; Marquez Diaz, F.; Guerrero Barrera, A.L.; Harel, J. Presence of multi-drug resistant pathogenic Escherichia coli in the San Pedro River located in the State of Aguascalientes, Mexico. *Front. Microbiol*. **2013**, *4*, 147.
35. Ramírez-Franco, J.H.; Galeano, L-A.; Vicente, M-A. Fly ash as photo-Fenton catalyst for the degradation of amoxicillin. *J. Environ. Chem. Eng*. **2019**, *7*, 103274.
36. Tavasol, F.; Tabatabaie, T.; Ramavandi, B.; Amiri, F. Design a new photocatalyst of sea sediment/titanate to remove cephalexin antibiotic from aqueous media in the presence of sonication/ultraviolet/hydrogen peroxide: Pathway and mechanism for degradation. *Ultrason. Sonochem.* **2020**, *65*, 105062.
37. Shojaei, M.; Esmaeili, H. Ultrasonic-assisted synthesis of zeolite/activated carbon@ MnO2 composite as a novel adsorbent for treatment of wastewater containing methylene blue and brilliant blue. *Environ. Monit. Assess.* **2022**, *194*, 279.
38. Tan, I.A.W.; Ahmad, A.L.; Hameed, B.H. Enhancement of basic dye adsorption uptake from aqueous solutions using chemically modified oil palm shell activated carbon. *Colloids Surf. A. Physicochem. Eng. Asp.* **2008**, *318*, 88-96.
39. Meng, J.; Cui, J.; Yu, S.; Jiang, H.; Zhong, C.; Hongshun, J. Preparation of aminated chitosan microspheres by one-pot method and their adsorption properties for dye wastewater. *Royal Soc. Open Sci.* **2019**, *6*, 182226.
40. Hui, K.C.; Suhaimi, H.; Sambudi, N.S. Electrospun-based TiO2 nanofibers for organic pollutant photodegradation: a comprehensive review. *Rev. Chem. Eng*. **2022**, *38*, 641-668.
41. Laskar, N.; Kumar, U. Adsorption of crystal violet from wastewater by modified bambusa tulda. *KSCE J. Civ. Eng*. **2018**, *22*, 2755-2763.
42. Wanyonyi, W.C.; Onyari, J.M.; Shiundu, P.M. Adsorption of Congo red dye from aqueous solutions using roots of Eichhornia crassipes: kinetic and equilibrium studies. *Energy Procedia* **2014**, *50*, 862-869.
43. Diantoro, M.; Kusumaatmaja, A.; Triyana, K. Study on photocatalytic properties of TiO2 nanoparticle in various pH condition. *J. Phys. Conf. Ser*. **2018**, *1011*, 012069.
44. Bakhtiari, R.; Kamkari, B.; Afrand, M.; Abdollahi, A. Preparation of stable TiO2-Graphene/Water hybrid nanofluids and development of a new correlation for thermal conductivity. *Powder Technol.* **2021**, *385*, 466-477.
45. Gatto, S. Photocatalytic activity assessment of micro-sized TiO2 used as powders and as starting material for porcelain gres tiles production. **2014**.
46. Sarafraz, M.; Sadeghi, M.; Yazdanbakhsh, A.; Amini, M.M.; Sadani, M.; Eslami, A. Enhanced photocatalytic degradation of ciprofloxacin by black Ti3+/N-TiO2 under visible LED light irradiation: Kinetic, energy consumption, degradation pathway, and toxicity assessment. *Process Saf. Environ. Prot.* **2020**, *137*, 261-272.
47. Inamuddin, I.; Asiri, A.M.; Lichtfouse, E. Nanophotocatalysis and environmental applications. Detoxification and Disinfection. Springer. **2020**, 30.
48. Lin, C.H.; Chen, W.H. Graphene Family Nanomaterials (GFN)-TiO2 for the Photocatalytic Removal of Water and Air Pollutants: Synthesis, Characterization, and Applications. *Nanomaterials* **2021**, *11*, 3195.
49. Neppolian, B.; Wang, Q.; Jung, H.; Choi, H. Ultrasonic-assisted sol-gel method of preparation of TiO2 nano-particles: characterization, properties and 4-chlorophenol removal application. *Ultrason. Sonochem.* **2008**, *15*, 649–658.
50. MODAN, E.M.; PLĂIAȘU, A.G. Advantages and disadvantages of chemical methods in the elaboration of nanomaterials. The Annals of "Dunarea de Jos" University of Galati. Fascicle IX, Metallurgy and Materials Science **2020**, *43*, 53-60.
51. Nyamukamba, P.; Okoh, O.; Mungondori, H.; Taziwa, R.; Zinya, S. Synthetic methods for titanium dioxide nanoparticles: a review. *Titanium dioxide-material for a sustainable environment* **2018**, 151-1755.
52. Madjene, F.; Aoudjit, L.; Igoud, S.; Lebik, H.; Boutra, B. A review: titanium dioxide photocatalysis for water treatment. *Transnational Journal of Science and Technology* **2013**, *3*, 1857-8047.
53. Otieno, S.; Lanterna, A.E.; Mack, J.; Derese, S.; Amuhaya, E.K.; Nyokong, T.; Scaiano, J.C. Solar Driven Photocatalytic Activity of Porphyrin Sensitized TiO2: Experimental and Computational Studies. *Molecules* **2021**, *26*, 3131.
54. Hernandez, J.V. Structural and Morphological modification of TiO2 doped metal ions and investigation of photo-induced charge transfer processes. Doctoral dissertation, Université du Maine; Instituto politécnico nacional, México **2017**.
55. Stamate, M.; Lazar, G. Application of titanium dioxide photocatalysis to create self-cleaning materials. *Romanian Technical Sciences Academy MOCM* **2007**, *13*, 280-285.
56. Fernandes, A.; Gągol, M.; Makoś, P.; Khan, J.A.; Boczkaj, G. Integrated photocatalytic advanced oxidation system (TiO2/UV/O3/H2O2) for degradation of volatile organic compounds. *Sep. Purif. Technol.* **2019**, *224*, 1-14.
57. Teoh, W.Y.; Urakawa, A.; Ng, Y.H.; Sit, P. Heterogeneous Catalysts: Advanced Design, Characterization, and Applications. *John Wiley & Sons*. **2021**.
58. Thomas, J.; Yoon, M. Facile synthesis of pure TiO2 (B) nanofibers doped with gold nanoparticles and solar photocatalytic activities. *Appl. Catal. B. Environ*. **2012**, *111*, 502-508.

59. Nguyen, V.H.; Tran, Q.B.; Nguyen, X.C.; Ho, T.T.T.; Shokouhimehr, M.; Vo, D.V.N.; Lam, S.S.; Nguyen, H.P.; Hoang, C.T.; Ly, Q.V.; Peng, W. Submerged photocatalytic membrane reactor with suspended and immobilized N-doped TiO2 under visible irradiation for diclofenac removal from wastewater. *Process Saf. Environ. Prot.* **2020**, *142*, 229-237.
60. Nakayama, N.; Hayashi, T. Preparation of TiO2 nanoparticles surface-modified by both carboxylic acid and amine: Dispersibility and stabilization in organic solvents. *Colloids Surf. A. Physicochem. Eng. Asp.* **2008**, *317*, 543-550.
61. Nuraje, N.; Asmatulu, R.; Mul, G. Green photo-active nanomaterials: sustainable energy and environmental remediation. *Royal Society of Chemistry* **2015**. https://doi.org/10.1039/9781782622642.
62. Amir, M.N.I.; Julkapli, N.M.; Bagheri, S.; Yousefi, A.T. TiO2 hybrid photocatalytic systems: impact of adsorption and photocatalytic performance. *Rev. Inorg. Chem.* **2015**, *35*, 151-178.
63. Arul, A.R.; Manjulavalli, T.E.; Venckatesh, R. Visible light proven Si doped TiO2 nanocatalyst for the photodegradation of Organic dye. *Mater. Today Proc.* **2019**, *18*, 1760-1769.
64. Janczarek, M.; Kowalska, E. On the origin of enhanced photocatalytic activity of copper-modified titania in the oxidative reaction systems. *Catalysts* **2017**, *7*, 317.
65. Jyothi, M.S.; Nayak, V.; Reddy, K.R.; Naveen, S.; Raghu, A.V. Non-metal (Oxygen, Sulphur, Nitrogen, Boron and Phosphorus)-Doped Metal Oxide Hybrid Nanostructures as Highly Efficient Photocatalysts for Water Treatment and Hydrogen Generation. *Nanophotocatalysis and Environmental Applications: Materials and Technology* **2019**, 83-105.
66. Rengaraj, S.; Li, X.Z. Enhanced photocatalytic activity of TiO2 by doping with Ag for degradation of 2, 4, 6-trichlorophenol in aqueous suspension. *J. Mol. Catal. A. Chem.* **2006**, *243*, 60-67.
67. Whang, T.J.; Huang, H.Y.; Hsieh, M.T.; Chen, J.J. Laser-induced silver nanoparticles on titanium oxide for photocatalytic degradation of methylene blue. *Int. J. Mol. Sci.* **2009**, *10*, 4707-4718.
68. Fang, T.; Yang, C.; Liao, L. Photoelectrocatalytic degradation of high COD dipterex pesticide by using TiO2/Ni photo electrode. *J. Environ. Sci.* **2012**, *24*, 1149–1156.
69. Khaoulani, S.; Chaker, H.; Cadet, C.; Bychkov, E.; Cherif, L.; Bengueddach, A.; Fourmentin, S. Wastewater treatment by cyclodextrin polymers and noble metal/mesoporous TiO2 photocatalysts. *C. R. Chim.* **2015**, *18*, 23–31.
70. Wang, R.; Tang, T.; Wei, Y.; Dang, D.; Huang, K.; Chen, X.; Yin, H.; Tao, X.; Lin, Z.; Dang, Z.; Lu, G. Photocatalytic debromination of polybrominated diphenyl ethers (PBDEs) on metal doped TiO2 nanocomposites: Mechanisms and pathways. *Environ. Int.* **2019**, *127*, 5–12.
71. Yadav, V.; Verma, P.; Sharma, H.; Tripathy, S.; Saini, V.K. Photodegradation of 4-nitrophenol over B-doped TiO2 nanostructure: effect of dopant concentration, kinetics, and mechanism. *Environ. Sci. Pollut. Res.* **2020**, *27*, 10966-10980.
72. Sescu, A.M.; Favier, L.; Lutic, D.; Soto-Donoso, N.; Ciobanu, G.; Harja, M. TiO2 doped with noble metals as an efficient solution for the photodegradation of hazardous organic water pollutants at ambient conditions. *Water* **2020**, *13*, 19.
73. Rekha, K.; Nirmala, M.; Nair, M.G.; Anukaliani, A. Structural, optical, photocatalytic and antibacterial activity of zinc oxide and manganese doped zinc oxide nanoparticles. *Phys. B. Condens. Matter.* **2010**, *405*, 3180-3185.
74. Espitia, P.J.P.; Soares, N.D.F.F.; Coimbra, J.S.D.R.; de Andrade, N.J.; Cruz, R.S.; Medeiros, E.A.A. Zinc oxide nanoparticles: synthesis, antimicrobial activity and food packaging applications. *Food Bioproc. Tech.* **2012**, *5*, 1447-1464.
75. Muruganandam, G.; Mala, N.; Pandiarajan, S.; Srinivasan, N.; Ramya, R.; Sindhuja, E.; Ravichandran, K. Synergistic effects of Mg and F doping on the photocatalytic efficiency of ZnO nanoparticles towards MB and MG dye degradation. *J. Mater. Sci. Mater.* **2017**, *28*, 18228-18235.
76. Coleman, V.A.; Jagadish, C. Basic properties and applications of ZnO. In Zinc oxide bulk, thin films and nanostructures. *Elsevier Science Ltd.* **2006**, pp. 1-20.
77. Shaba, E.Y.; Jacob, J.O.; Tijani, J.O.; Suleiman, M.A.T. A critical review of synthesis parameters affecting the properties of zinc oxide nanoparticle and its application in wastewater treatment. *Appl. Water Sci.* **2021**, *11*, 48.
78. Saedy, S.; Haghighi, M.; Amirkhosrow, M. Hydrothermal synthesis and physicochemical characterization of CuO/ZnO/Al2O3 nanopowder. Part I: Effect of crystallization time. *Particuology* **2012**, *10*, 729-736.
79. Lee, Y.C.; Yang, C.S.; Huang, H.J.; Hu, S.Y.; Lee, J.W.; Cheng, C.F.; Huang, C.C.; Tsai, M.K.; Kuang, H.C. Structural and optical properties of ZnO nanopowder prepared by microwave-assisted synthesis. *J. Lumin* **2010**, *130*, 1756-1759.
80. Pasang, T.; Namratha, K.; Parvin, T.; Ranganathaiah, C.; Byrappa, K. Tuning of band gap in TiO2 and ZnO nanoparticles by selective doping for photocatalytic applications. *Mater. Res. Innov.* **2015**, *19*, 73-80.
81. Asgari, E.; Esrafili, A.; Jafari, A.J.; Kalantary, R.R.; Nourmoradi, H.; Farzadkia, M. The comparison of ZnO/polyaniline nanocomposite under UV and visible radiations for decomposition of metronidazole: degradation rate, mechanism and mineralization. *Process Saf. Environ. Prot.* **2019**, *128*, 65-76.

82. Wang, Y.; Yang, C.; Liu, Y.; Fan, Y.; Dang, F.; Qiu, Y.; Zhou, H.; Wang, W.; Liu, Y. Solvothermal Synthesis of ZnO Nanoparticles for Photocatalytic Degradation of Methyl Orange and p-Nitrophenol. *Water* **2021**, *13*, 3224.
83. Berjilia, M.M.; Manikandan, S.; Dhanalakshm, K.B. PHOTOCATALYTIC DEGRADATION OF RESORCINOL OVER ZnO POWDER THE INFLUENCE OF PEROXOMONOSULPHATE AND PEROXODISULPHATE ON THE REACTION RATE. *Int. J. Adv. Res*. **2016**, *4*, 1316-1323.
84. Lofrano, G.; Libralato, G.; Brown, J. Nanotechnologies for environmental remediation. *Springer International Publishing*. **2017**.
85. Jeong, J.H.; Hong, K.; Kwon, S.H.; Lim, D.C. Development of Inverted Organic Photovoltaics with Anion doped ZnO as an Electron Transporting Layer. *Journal of the Korean Institute of Surface Engineering* **2016**, *49*, 490-497.
86. Kim, S.; Jeong, J.; Hoang, Q.V.; Han, J.W. A. Prasetio, M. Jahandar, Y.H. Kim, S. Cho, D.C. Lim, The role of cation and anion dopant incorporated into a ZnO electron transporting layer for polymer bulk heterojunction solar cells. *RSC Adv.* **2019**, *9*, 37714-37723.
87. Güy, N.; Çakar, S.; Özacar, M. Comparison of palladium/zinc oxide photocatalysts prepared by different palladium doping methods for congo red degradation. *J. Colloid Interface Sci*. **2016**, *466*, 128-137.
88. Kuzhalosai, V.; Subash, B.; Senthilraja, A.; Dhatshanamurthi, P.; Shanthi, M. Synthesis, characterization and photocatalytic properties of SnO2–ZnO composite under UV-A light, Spectrochim. *Acta A. Mol. Biomol. Spectrosc*. **2013**, *115*, 876-882.
89. Adeel, M.; Saeed, M.; Khan, I.; Muneer, M.; Akram, N. Synthesis and characterization of Co–ZnO and evaluation of its photocatalytic activity for photodegradation of methyl orange. *ACS Omega* **2021**, *6*, 1426-1435.
90. Vallejo, W.; Cantillo, A.; Díaz-Uribe, C. Methylene blue photodegradation under visible irradiation on Ag-doped ZnO thin films. *Int. J. Photoenergy* **2020**, *2020*.
91. Vallejo, W.; Cantillo, A.; Salazar, B.; Diaz-Uribe, C.; Ramos, W.; Romero, E.; Hurtado, M. Comparative study of ZnO thin films doped with transition metals (Cu and Co) for methylene blue photodegradation under visible irradiation. *Catalysts* **2020**, *10*, 528.
92. Alkallas, F.H.; Ben Gouider Trabelsi, A.; Nasser, R.; Fernandez, S.; Song, J.M.; Elhouichet, H. Promising Cr-Doped ZnO Nanorods for Photocatalytic Degradation Facing Pollution. *Appl. Sci*. **2021**, *12*., 34.
93. Ragupathy, S.; Priyadharsan, A.; AlSalhi, M.S.; Devanesan, S.; Guganathan, L.; Santhamoorthy, M.; Kim, S.C. Effect of doping and loading Parameters on photocatalytic degradation of brilliant green using Sn doped ZnO loaded CSAC. *Environ. Res.* **2022**, *210*, 112833.
94. Tzewei, T.; Ibrahim, A.H.; Abidin, C.Z.A.; Ridwan, F.M. The effect of iron doping on ZnO catalyst on dye removal efficiency. *IOP Conf. Ser. Earth Environ. Sci.* **2020**, *476*, 012108.
95. Kong, J.Z.; Li, A.D.; Li, X.Y.; Zhai, H.F.; Zhang, W.Q.; Gong, Y.P.; Li, H.; Wu, D. Photo-degradation of methylene blue using Ta-doped ZnO nanoparticle. *J. Solid State Chem.* **2010**, *183*, 1359-1364.
96. Prabakaran, E.; Pillay, K. Synthesis of N-doped ZnO nanoparticles with cabbage morphology as a catalyst for the efficient photocatalytic degradation of methylene blue under UV and visible light. *RSC Adv.* **2019**, *9*, 7509-7535.
97. Wu, C.; Zhang, Y.C.; Huang, Q. Solvothermal synthesis of N-doped ZnO microcrystals from commercial ZnO powder with visible light-driven photocatalytic activity. *Mater. Lett*. **2014**, *119*, 104-106.
98. Yi-hao, T.; Hang, Z.; Yin, W.; Ming-hui, D.; Guo, J.; Bin, Z. Facile fabrication of nitrogen-doped zinc oxide nanoparticles with enhanced photocatalytic performance. *Micro. Nano. Lett*. **2015**, *10*, 432-434.
99. Li, B.; Liu, T.; Wang, Y.; Wang, Z. ZnO/graphene-oxide nanocomposite with remarkably enhanced visible-light-driven photocatalytic performance. *J. Colloid Interface Sci.* **2012**, *377*, 114-121.
100. Fu, D.; Han, G.; Chang, Y.; Dong, J. The synthesis and properties of ZnO–graphene nano hybrid for photodegradation of organic pollutant in water. *Mater. Chem. Phys*. **2012**, *132*, 673-681.
101. Bechambi, O.; Sayadi, S.; Najjar, W. Photocatalytic degradation of bisphenol A in the presence of C-doped ZnO: effect of operational parameters and photodegradation mechanism. *J. Ind. Eng. Chem.* **2015**, *32*, 201-210.
102. Li, X.; Wang, Q.; Zhao, Y.; Wu, W.; Chen, J.; Meng, H. Green synthesis and photo-catalytic performances for ZnO-reduced graphene oxide nanocomposites. *J. Colloid Interface Sci.* **2013**, *411*, 69-75.
103. Zhang, Y.; Park, M.; Kim, H-Y.; El-Newehy, M.; Rhee, K.Y.; Park, S-J. Effect of TiO2 on photocatalytic activity of polyvinylpyrrolidone fabricated via electrospinning. *Compos. B. Eng*. **2015**, *80*, 355–360.
104. Notodarmojo, S.; Sugiyana, D.; Handajani, M.; Kardena, E.; Larasati, A. Synthesis of TiO2 nanofiber-nanoparticle composite catalyst and its photocatalytic decolorization performance of reactive black 5 dye from aqueous solution. *J. Eng. Technol. Sci.* **2017**, *49*, 3.
105. Saiful Amran, S.N.B.; Wongso, V.; Abdul Halim, N.S.; Husni, M.K.; Sambudi, N.S.; Wirzal, M.D.H. Immobilized carbondoped TiO2 in polyamide fibers for the degradation of methylene blue. *J. Asian Ceram. Soc.* **2019**, *7*, 321–330.

 doi:10.20944/preprints202406.0592.v1

106. Erdemoğlu, S.; Aksu, S.K.; Sayılkan, F.; Izgi, B.; Asiltürk, M.; Sayılkan, H.; Frimmel, F.; Güçer, Ş. Photocatalytic degradation of Congo Red by hydrothermally synthesized nanocrystalline TiO2 and identification of degradation products by LC–MS. *J. Hazard. Mater.* **2008**, *155*, 469-476.
107. Xiang, Q.; Yu, J.; Jaroniec, M. Enhanced photocatalytic H 2-production activity of graphene-modified titania nanosheets. *Nanoscale* **2011**, *3*, 3670-3678.
108. Fan, H.; Wu, R.; Liu, H.; Yang, X.; Sun, Y.; Chen, C. Synthesis of metal-phase-assisted 1T@ 2H-MoS2 nanosheet-coated black TiO2 spheres with visible light photocatalytic activities. *J. Mater. Sci.* **2018**, *53*, 10302-10312.
109. Xia, T.; Wang, Y.; Mai, C.; Pan, G.; Zhang, L.; Zhao, W.; Zhang, J. Facile in situ growth of ZnO nanosheets standing on Ni foam as binder-free anodes for lithium ion batteries. *RSC Adv.* **2019**, *9*, 19253-19260.
110. Guo, L.; Ji, Y.L.; Xu, H.; Simon, P.; Wu, Z. Regularly shaped, single-crystalline ZnO nanorods with wurtzite structure. *J. Am. Chem. Soc.* **2002**, *124*, 14864-14865.
111. Zhou, Q.; Xie, B.; Jin, L.; Chen, W.; Li, J. Hydrothermal Synthesis and Responsive Characteristics of Hierarchical Zinc Oxide Nanoflowers to Sulfur Dioxide. *J. Nanotechnol*. **2016**.
112. Li, Q.; Wang, Q.; Chen, Z.; Ma, Q.; An, M. A facile and flexible approach for large-scale fabrication of ZnO nanowire film and its photocatalytic applications. *Nanomaterials* **2019**, *9*, 846.
113. Srivastava, R.R.; Kumar Vishwakarma, P.; Yadav, U.; Rai, S.; Umrao, S.; Giri, R.; Saxena, P.S.; Srivastava, A. 2D SnS2 Nanostructure-Derived Photocatalytic Degradation of Organic Pollutants Under Visible Light. *Front. Nanotechnol.* **2021**, *3*, 711368.
114. Tayeb, A.M.; Hussein, D.S. Synthesis of TiO2 nanoparticles and their photocatalytic activity for methylene blue. *American Journal of Nanomaterials* **2015**, *3*, 57-63.
115. Tawfik, A.; Alalm, M.G.; Awad, H.M.; Islam, M.; Qyyum, M.A.; Al-Muhtaseb, A.A.H.; Osman, A.I.; Lee, M. Solar photo-oxidation of recalcitrant industrial wastewater: a review. *Environ. Chem. Lett.* **2022**, *20*, 1839–1862.
116. Parida, K.M.; Parija, S. Photocatalytic degradation of phenol under solar radiation using microwave irradiated zinc oxide. *Sol. Energy* **2006**, *80*, 1048–1054.
117. Benhabiles, O.; Mahmoudi, H.; Lounici, H.; Goosen, M.F. Effectiveness of a photocatalytic organic membrane for solar degradation of methylene blue pollutant. *Desalin. Water Treat.* **2016**, *57*, 14067-14076.
118. Shelar, S.G.; Mahajan, V.K.; Patil, S.P.; Sonawane, G.H. Effect of doping parameters on photocatalytic degradation of methylene blue using Ag doped ZnO nanocatalyst. *SN Appl. Sci.* **2020**, *2*, 820.
119. Mohsenzadeh, M.; Mirbagheri, S.A.; Sabbaghi, S. Degradation of 1,2-dichloroethane by photocatalysis using immobilized PAni-TiO_2 nano-photocatalyst. *Environ. Sci. Pollut. Res.* **2019**, *26*, 31328–31343.
120. Hameed, B.H.; Salman, J.M.; Ahmad, A.L. Adsorption isotherm and kinetic modeling of 2,4-D pesticide on activated carbon derived from date stones. *J. Hazard. Mater.* **2009**, *163*, 121-126.
121. Lopez-Alvarez, B.; Torres-Palma, R.A.; Penuela, G. Solar photocatalitycal treatment of carbofuran at lab and pilot scale: effect of classical parameters, evaluation of the toxicity and analysis of organic by-products. *J. Hazard. Mater.* **2011**, *191*, 196–203.
122. Saien, J.; Khezrianjoo, S. Degradation of the fungicide carbendazim in aqueous solutions with UV/TiO2 process: optimization, kinetics and toxicity studies. *J. Hazard. Mater*. **2008**, *157*, 269–276.
123. Elmolla, E.S.; Chaudhuri, M. Degradation of amoxicillin, ampicillin and cloxacillin antibiotics in aqueous solution by the UV/ZnO photocatalytic process. *J. Hazard. Mater*. **2010**, *173*, 445–449.
124. Whyte, H.E. Evaluation of the performance of photocatalytic systems for the treatment of indoor air in medical environments. Doctoral dissertation, Ecole nationale supérieure Mines-Télécom Atlantique **2018**.
125. Lee, K.M.; Lai, C.W.; Ngai, K.S.; Juan, J.C. Recent developments of zinc oxide based photocatalyst in water treatment technology: a review. *Water Res.* **2016**, *88*, 428-448.
126. Elaziouti, A.; Ahmed, B. ZnO-assisted photocatalytic degradation of congo Red and benzopurpurine 4B in aqueous solution. *J. Chem. Eng. Process. Technol.* **2011**, *2*, 1-9.
127. Gómez-López, V.M.; Koutchma, T.; Linden, K. Ultraviolet and pulsed light processing of fluid foods, In Novel thermal and non-thermal technologies for fluid foods. *Academic Press*. **2012**, 185-223.
128. Bayarri, B.; Abellán, M.N.; Giménez, J.; Esplugas, S. Study of the wavelength effect in the photolysis and heterogeneous photocatalysis. *Catal. Today* **2007**, *129*, 231-239.
129. Nilsson, A. Removal of formaldehyde from industrial waste water. M.Sc. thesis in Chemical Engineering, CHALMERS UNIVERSITY OF TECHNOLOGY, Sweden **2020**.
130. Chen, Y.W.; Hsu, Y.H. Effects of reaction temperature on the photocatalytic activity of TiO2 with Pd and Cu cocatalysts. *Catalysts* **2021**, *11*, 966.
131. Hu, Q.; Liu, B.; Song, M.; Zhao, X. Temperature effect on the photocatalytic degradation of methyl orange under UV-vis light irradiation. *Journal of Wuhan University of Technology-Mater. Sci. Ed*. **2010**, *25*, 210-213.
132. Barakat, N.A.; Kanjwal, M.A.; Chronakis, I.S.; Kim, H.Y. Influence of temperature on the photodegradation process using Ag-doped TiO2 nanostructures: negative impact with the nanofibers. *J. Mol. Catal. A. Chem.* **2013**, *366*, 333-340.

133. Shi, X.; Zhang, X.; Ma, L.; Xiang, C.; Li, L. TiO2-Doped chitosan microspheres supported on cellulose acetate fibers for adsorption and photocatalytic degradation of methyl orange. *Polymers* **2019**, *11*, 1293.
134. Zayed, M.; Samy, S.; Shaban, M.; Altowyan, A.S.; Hamdy, H.; Ahmed, A.M. Fabrication of TiO2/NiO pn nanocomposite for enhancement dye photodegradation under solar radiation. *Nanomaterials* **2022**, *12*, 989.
135. Nikoofar, K.; Haghighi, M.; Lashanizadegan, M.; Ahmadvand, Z. ZnO nanorods: efficient and reusable catalysts for the synthesis of substituted imidazoles in water. *J. Taibah. Univ. Sci*. **2015**, *9*, 570-578.
136. Wang, X.; Jin, H.; Wu, D.; Nie, Y.; Tian, X.; Yang, C.; Zhou, Z.; Li, Y. Fe3O4@ S-doped ZnO: A magnetic, recoverable, and reusable Fenton-like catalyst for efficient degradation of ofloxacin under alkaline conditions. *Environ. Res*. **2020**, *186*, 109626.
137. Ikram, M.; Aslam, S.; Haider, A.; Naz, S.; Ul-Hamid, A.; Shahzadi, A.; Ikram, M.; Haider, J.; Ahmad, S.O.A.; Butt, A.R. Doping of Mg on ZnO nanorods demonstrated improved photocatalytic degradation and antimicrobial potential with molecular docking analysis. *Nanoscale Res. Lett.* **2021**, *16*, 78.
138. Padikkaparambil, S.; Narayanan, B.; Yaakob, Z.; Viswanathan, S.; Tasirin, S.M. Au/TiO2 reusable photocatalysts for dye degradation. *Int. J. Photoenergy* **2013**, 2013.
139. Wu, Q.; Zhang, Z. The preparation of self-floating Sm/N co-doped TiO_2/diatomite hybrid pellet with enhanced visible-light-responsive photoactivity and reusability. *Adv. Powder Technol.* **2019**, *30*, 415-422.
140. Song, L.; Jing, W.; Chen, J.; Zhang, S.; Zhu, Y.; Xiong, J. High reusability and durability of carbon-doped TiO2/carbon nanofibrous film as visible-light-driven photocatalyst. *J. Mater. Sci.* **2019**, *54*, 3795-3804.
141. Bahrudin, N.N.; Nawi, M.A.; Nawawi, W.I. Enhanced photocatalytic decolorization of methyl orange dye and its mineralization pathway by immobilized TiO2/polyaniline. *Res. Chem. Intermed.* **2019**, *45*, 2771-2795.
142. Moosavi, S.; Li, R.Y.M.; Lai, C.W.; Yusof, Y.; Gan, S.; Akbarzadeh, O.; Chowhury, Z.Z.; Yue, X.G.; Johan, M.R. Methylene blue dye photocatalytic degradation over synthesised Fe3O4/AC/TiO2 nano-catalyst: degradation and reusability studies. *Nanomaterials* **2020**, *10*, 2360.
143. Ma, L.; Chen, Y.; Zheng, J. An efficient, stable and reusable polymer/TiO2 photocatalytic membrane for aqueous pollution treatment. *J. Mater. Sci.* **2021**, *56*, 11335-11351.
144. Yeganeh-Faal, A.; Bordbar, M.; Negahdar, N.; Nasrollahzadeh, M. Green synthesis of the Ag/ZnO nanocomposite using Valeriana officinalis L. root extract: application as a reusable catalyst for the reduction of organic dyes in a very short time. *IET Nanobiotechnol.* **2017**, *11*, 669-676.
145. Mansoori, G.A.; Bastami, T.R.; Ahmadpour, A.; Eshaghi, Z. Environmental application of nanotechnology. *Annu. Rev. Nano. Res.* **2008**, *2*, 439–493.
146. Baaloudj, O.; Nasrallah, N.; Bouallouche, R.; Kenfoud, H.; Khezami, L.; Assadi, A.A. High efficient Cefixime removal from water by the sillenite Bi12TiO20: Photocatalytic mechanism and degradation pathway. *J. Clean. Prod.* **2022**, *330*, 129934.
147. Zhang, Y.Z.; Wang, X.; Feng, Y.; Li, J.; Lim, C.T.; Ramakrishna, S. Coaxial electrospinning of (fluorescein isothiocyanate-Conjugated bovine serum albumin)-Encapsulated poly ("-caprolactone) nanofibers for sustained release. *Biomacromolecule* **2006**, *7*, 1049–1057.
148. Chuang, C.S.; Wang, M.K.; Ko, C.H.; Ou, C.C.; Wu, C.H. Removal of benzene and toluene by carbonized bamboo materials modified with TiO2. *Bioresour. Technol*. **2008**, *99*, 954–958.
149. Hou, X.; Cai, Y.; Song, X.; Wu, Y.; Zhang, J.; Wei, Q. Electrospun TiO2 nanofibers coated with polydopamine for enhanced sunlight-driven photocatalytic degradation of cationic dyes. *Surf. Interface Anal*. **2019**, *51*, 169–176.
150. Baaloudj, O.; Assadi, A.A.; Azizi, M.; Kenfoud, H.; Trari, M.; Amrane, A.; Assadi, A.A.; Nasrallah, N. Synthesis and characterization of ZnBi2O4 nanoparticles: photocatalytic performance for antibiotic removal under different light sources. *Appl. Sci.* **2021**, *11*, 3975.
151. Norouzi, M.; Fazeli, A.; Tavakoli, O. Photocatalytic degradation of phenol under visible light using electrospun Ag/TiO2 as a 2D nano-powder: Optimizing calcination temperature and promoter content. *Adv. Powder Technol*. **2022**, *33*, 103792.
152. Chiang, Y.J.; Lin, C.C. Photocatalytic decolorization of methylene blue in aqueous solutions using coupled ZnO/SnO2 photocatalysts. *Powder Technol*. **2013**, *246*, 137-143.